DOI: 10.1534/genetics.109.107748

A Gain-of-Function Screen Identifying Genes Required for Growth and Pattern Formation of the *Drosophila melanogaster* Wing

Cristina Cruz, Alvaro Glavic,[1] Mar Casado and Jose F. de Celis[2]

Centro de Biología Molecular "Severo Ochoa" (CBMSO), Consejo Superior de Investigaciones Científicas and Universidad Autónoma de Madrid, Cantoblanco, Madrid 28049, Spain

Manuscript received July 25, 2009
Accepted for publication September 3, 2009

ABSTRACT

The *Drosophila melanogaster* wing is a model system for analyzing the genetic control of organ size, shape, and pattern formation. The formation of the wing involves a variety of processes, such as cell growth, proliferation, pattern formation, and differentiation. These developmental processes are under genetic control, and many genes participating in specific aspects of wing development have already being characterized. In this work, we aim to identify novel genes regulating wing growth and patterning. To this end, we have carried out a gain-of-function screen generating novel P-UAS (upstream activating sequences) insertions allowing forced gene expression. We produced 3340 novel P-UAS insertions and isolated 300 that cause a variety of wing phenotypes in combination with a Gal4 driver expressed exclusively in the central domain of the presumptive wing blade. The mapping of these P-UAS insertion sites allowed us to identify the gene that causes the gain-of-function phenotypes. We show that a fraction of these phenotypes are related to the induction of cell death in the domain of ectopic gene expression. Finally, we present a preliminary characterization of a gene identified in the screen, the function of which is required for the development of the L5 longitudinal vein.

SEVERAL characteristics make the Drosophila wing a suitable model system for studying the genetic and cellular bases of epithelial development. In particular, the wing has a constant size, shape, and pattern of veins and sensory organs, the formation of which is under tight genetic control, and many of the genes and mechanisms involved in the development of the wing have already being identified (Blair 1995; Mann and Morata 2000; de Celis 2003). The wing is also very sensitive to genetic manipulations, and changes in the level or pattern of gene expression alter wing morphology and pattern in a way that is informative about the developmental process affected (Molnar *et al.* 2006). Furthermore, the activities of conserved signaling pathways play a fundamental role in controlling wing growth and patterning, and conventional phenotypic analysis allows the identification of additional components of these pathways (Molnar *et al.* 2006).

The wing develops from an epithelial tissue, the wing imaginal disc, which grows during larval development to acquire its final size and cell number in the first hours of pupal development (Bate and Martinez-Arias 1991; Cohen 1993; Milan *et al.* 1996). As the disc increases its size by cell proliferation, the activities of the Decapentaplegic (Dpp), Hedgehog (Hh), and Wingless (Wg) pathways subdivide the epithelium into domains of gene expression that correspond to particular wing territories and cell types (Zecca *et al.* 1995; Lawrence and Struhl 1996). These signaling pathways have in common that their ligands are secreted proteins that act at a distance from the source of secretion to activate their respective transduction pathways, which regulates the expression of downstream genes in large cellular domains (Struhl and Basler 1993). In summary, Hh protein is secreted by all cells belonging to the posterior compartment and activates its targets only in anterior cells close to the anterior/posterior compartment boundary (Tabata and Kornberg 1994; Strigini and Cohen 1997; Méthot and Basler 1999; Ingham and McMahon 2001). Different levels of Hh signaling regulate different target genes, and in this manner Hh activity subdivides the center of the wing disc into expression domains corresponding to the L3/L4 proveins and the L3/L4 intervein (Vervoort *et al.* 1999; Mohler *et al.* 2000). In addition to patterning the central wing-disc region, Hh signaling also regulates the expression of Dpp in a stripe of anterior cells, and Dpp, in turn, activates its pathway in a broad domain of cells centered along the anterior/posterior boundary (de Celis *et al.* 1996a; Nellen *et al.* 1996; Tsuneizumi *et al.* 1997). The activity of Dpp is required for the growth of

Supporting information is available online at http://www.genetics.org/cgi/content/full/genetics.109.107748/DC1.

[1]*Present address:* Center for Genomics of the Cell, Faculty of Sciences, University of Chile, Las Palmeras 3425, Santiago, Chile.

[2]*Corresponding author:* CBMSO, c/ Nicolás Cabrera 1, Cantoblanco, Madrid 28049, Spain. E-mail: jfdecelis@cbm.uam.es

the disc and for the patterning and differentiation of all longitudinal veins. The expression of *wg* is restricted in the wing blade to dorsal and ventral cells abutting the dorso-ventral compartment boundary, and Wg protein secreted from this narrow domain contributes to the formation of the wing margin (Struhl and Basler 1993; Rulifson and Blair 1995; Diaz-Benjumea and Cohen 1995; de Celis *et al.* 1996b; Zecca *et al.* 1996; Micchelli *et al.* 1997). Finally, the position of the longitudinal veins is established in the wing epithelium using the positional information coordinates laid out by the Hh, Dpp, and Wg pathways. In this process, the activities of the EGFR and Notch signaling pathways play a central role defining and restricting, respectively, the specification of vein cells (de Celis 1998).

Although we have a detailed description of imaginal wing-disc growth, its pattern of cell divisions, the spatial domains and mechanisms of signaling, and the identity of some transcriptional regulators that contribute to wing development and vein formation, it is not fully known how these processes are integrated to generate the wing. In particular, the mechanisms contributing to regulate organ size and shape are still largely unknown. It is likely that part of this problem is that many genes participating in wing growth have not yet been identified, and therefore it is expected that further genetic screens are needed to identify these missing elements. The best criteria to detect genes involved in wing development are the expression pattern and the loss-of-function phenotype, and different strategies using these parameters have already being used with success to isolate such genes (Calleja *et al.* 1996; Walsh and Brown 1998; Butler *et al.* 2003). However, loss-of-function screens have several drawbacks that have prevented its systematic use in adult tissues. Thus, mutant alleles can be cell lethal, preventing the observation of phenotypes in the adult, and mapping novel mutations to individual genes is still problematic and time-consuming. As a complementary approach, the identification of genes affecting wing formation relies on gain-of-function screens, which are carried out using modified transposable elements carrying yeast UAS sequences (Rørth 1996; Toba *et al.* 1999). Thus, it has been observed that increased or ectopic gene expression causes phenotypes that are informative about the normal function of the gene, and the analysis of these phenotypes might uncover genes that, due to functional redundancy, are not easily found in loss-of-function screens (Molnar *et al.* 2006).

In this work, we present the results of a gain-of-function screen aiming to identify genes involved in wing growth and pattern formation. We used a Gal4 driver expressed only in a central domain of the wing disc and combined it with newly generated insertions of a *P* element containing UAS sequences (*P-GS* element) (Toba *et al.* 1999). Among 3340 new *P-GS* insertions, we isolated 300 that cause alterations in the differentiation of the veins and/or the general morphology of the wing. The molecular mapping of the *P*-element insertion sites identified 245 insertion sites with 287 candidate genes, including many known genes belonging to the signaling pathways affecting wing development, and a large fraction (32%) of previously uncharacterized coding sequences (CGs). One of the identified insertions corresponds to *CG3998*, and we show that its function is required for the regulation of the expression of the Iroquois genes in the longitudinal vein L5 and for the formation of this vein. Interestingly, a fraction of the phenotypes caused by overexpression are caused in part by the induction of cell death by inappropriate activation of the JNK signaling pathway.

MATERIALS AND METHODS

Drosophila stocks: We used the stocks *y w;* Δ*2-3 Dr/TM2* and *w; CyO P-GS/If* to carry out the screen, and the Gal4 lines *Gal4-638*, *Gal4-shv* (Sotillos and de Celis 2006), *Gal4-ey* (Halder *et al.* 1998), and *Gal4-253* (de Celis *et al.* 1999) to drive gene expression in particular domains of the antenna-eye and wing discs. We also used the following UAS lines: *UAS-GFP* (Ito *et al.* 1997), *UAS-N^{fcd}* (Lawrence *et al.* 2000), *UAS-rho* and *UAS-Ni* (de Celis *et al.* 1997), *UAS-dad* (Tsuneizumi *et al.* 1997), *UAS-dpp* (Staehling-Hampton *et al.* 1994), *UAS-dpp-GFP* (Teleman and Cohen 2000), *UAS-EGFR^{DN}*, *UAS-ras^{V12}* (Buff *et al.* 1998), *UAS-puc^{2A}* (Martin-Blanco *et al.* 1998), *UAS-hippo*, *UAS-hep*, the UAS RNA interference (RNAi) line 3998R2 and the insertions *P{lacW}zf30C^{k02506}*, *P{EP}zf30C^{EP2228}*, and *l(2)SH1998^{SH1998}* (Bloominton and Szeged stock centers). Unless otherwise stated, crosses were done at 25°. Wings were mounted in lactic acid–ethanol (1:1) and photographed with a Spot digital camera and a Zeiss Axioplan microscope. Lines not described in the text can be found in FlyBase (Wilson *et al.* 2008).

Generation of new *P-GS* insertions: We used Δ*2-3* as a source of transposase to mobilize a *P-GS* element placed in a CyO chromosome in a *w* background (Figure 1A). Males carrying *CyO*, *P-GS*, and Δ*2-3* were crossed with homozygous *w* females. The w$^+$ CyO$^+$ progeny were crossed in groups of 5–10 w$^+$ individuals with *Gal4-sal^{EPv}* flies, and the progeny of these crosses were scored to identify wing phenotypes. Individual stocks were established using the stocks *w; CyO/Gal4-sal^{EPv}* and *w; TM6b/TM2* (see Figure 1A for a summary of the crosses). The *Gal4-sal^{EPv}* driver (Figure 1C) is expressed in the central region of the wing blade during the third larval stage (Figure 1, B and C).

Molecular mapping of novel *P-GS* insertions: To identify the insertion site of each *P-GS*, we extracted genomic DNA from 30 frozen flies that were kept for at least 1 day at −80°. Genomic DNA was isolated following standard procedures in 150 μl Tris–HCl 10 mm, pH 7.5. Five microliters of genomic DNA was digested 4 hr at 37° with either *Hha*I or *Msp*I. Following heat inactivation of the enzymes by a 20-min incubation at 65°, 5 μl of each digestion were incubated for 2 hr at room temperature with T4 ligase in a final volume of 200 μl. We used 5 μl of ligation reaction in 50 μl to set inverse-PCR reactions using the 3′ P-specific oligonucleotides CTTCTTGGCAGATTTCAGTAGTTGC and ATTGCAAGCA TACGTTAAGTGGA or the 5′ P-specific oligonucleotides CTTCTTGGCAGATTTCAGTAGTTGC and GTGTATACTTC GGTAAGCTTCG. The PCR parameters were the following: 95° for 5 min, 35 cycles; 95° for 45 sec, 55° for 1 min, 72° for

2 min, and a 10-min extension at 72°. The PCR products were visualized in agarose 1%, purified using the Promega PCR-purification kit and sequenced with the oligonucleotide CGACGGGACCACCTTATGTTA. The resulting sequences were searched in the NCBI database, and the adjacent genes were annotated (see supporting information, Table S1).

Generation of *Gal4-salEPv*: To generate the *Gal4-sal^{EPv}* driver, we cloned a 1080-base pairs fragment from the *sal* enhancer (sal^{EPv}) (Barrio and de Celis 2004) into pW8-Gal4 (Brand and Perrimon 1993).

Immunocytochemistry: Wings discs were dissected, fixed, and stained as described in de Celis *et al.* (1997). To detect apoptotic cells, we used antiactivated Caspase 3 (1:200 Cell Signaling). Secondary antibodies were from Jackson Immunological Laboratories (used at 1/200 dilution). Confocal images were captured using a BioRad confocal microscope.

***In situ* hybridization:** We used dygoxigenin-labeled RNA probes synthesized from the corresponding EST clones. Third instar larvae were dissected in PBS and fixed 30 min in 4% paraformaldehyde, washed three times for 5 min in PBS-0.1% Tween20, and refixed for 20 min in paraformaldehyde 4% + 0.1% Tween20. After several washes in PBS-0.1% Tween20, the carcases were kept at −20° in hybridization solution (HS: 50% formamide, SSC 5×, 100 μg/ml salmon sperm DNA, 50 μg/ml heparine, 0.1% Tween20). The hybridization was carried out overnight at 55° with 2 μl of probe in 100 μl of HS (previously denatured by a 10-min incubation at 80°). Excess probe was washed at 55° in HS, and discs were washed several times in PBS-0.1% Tween20; afterward they were incubated for 2 hr with antidigoxigenine antibody (Roche) in a 1:4000 dilution in PBS-0.1% Tween20-1% BSA. The color reaction was carried out in 100 mm NaCl, 50 mm MgCl2, 100 mm Tris–HCl, pH 9.5, 0.1% Tween20, nitroblue tetrazolium chloride, and bromo-chloro-indolyl-phosphate (Roche). After the color developed, discs were rinsed several times in PBS-0.1% Tween20, dissected in 30% glycerol, and mounted in 70% glycerol.

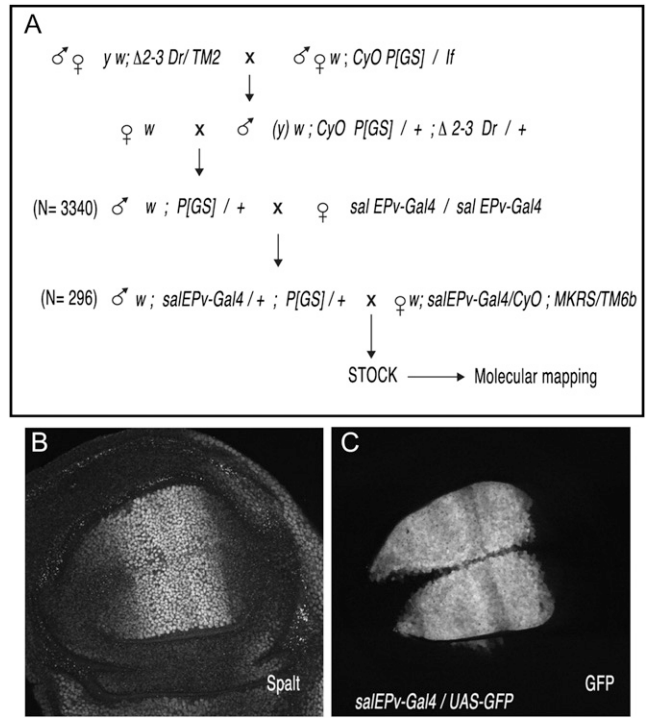

Figure 1.—Schematic of genetic crosses used to generate and select novel *P-GS* insertions and expression pattern of the *sal^{EPv}-Gal4* driver. (A) Generation of new *P-GS* insertions using Δ2-3 transposase to mobilize a *P-GS* element inserted in a *CyO* chromosome (*CyO P[GS]*). Males and females with novel *P-GS* insertion [*w; P(GS)/+*; $n = 3340$] were crossed to *sal^{EPv}-Gal4* flies to induce the expression of the genes adjacent to the *P-GS* insertion site, and flies with a mutant wing phenotype [*w; sal^{EPv}-Gal4/+; P[GS]/+*; $n = 296$] were selected to establish balanced lines (STOCK). (B) Expression of Spalt protein (Spalt) in the wing region of a late L3 wing imaginal disc. (C) Expression of green fluorescent protein (GFP) in *sal^{EPv}-Gal4/UAS-GFP* wing imaginal discs. The expression is restricted to the central domain of the wing blade.

RESULTS

We aimed to identify genes that, when overexpressed, modify the pattern of veins and/or the size and shape of the wing. Because we sought to screen newly generated P-UAS insertions in a F_1 generation, the combination between the Gal4 driver and any UAS line should be viable and fertile. To choose a suitable Gal4 line and visualize the phenotypes resulting from modifications in the signaling pathways regulating wing development, we forced the expression of several members of the Dpp, EGFR, and Notch pathways in the wing disc using a variety of Gal4 lines expressed in the wing blade such as *nubbin-Gal4* (Calleja *et al.* 1996), *spalt-Gal4* (Barrio *et al.* 1999), and *638-Gal4* (Molnar *et al.* 2006). The resulting Gal4/UAS combinations generally displayed late pupal lethality, with some escapers showing severe phenotypes in the wing (data not shown). The lethality in the pupal stage of these Gal4/UAS combinations precluded us from using Gal4 lines with generalized expression in the wing for the screening, and we decided to generate a novel Gal4 line expressed exclusively in a restricted domain of the wing blade. To this end, we made the *sal^{EPv}-Gal4* construct by cloning the regulatory region driving *spalt* expression in the wing blade (Barrio and de Celis 2004) with the coding region of Gal4 (Brand and Perrimon 1993). The expression of GFP in *sal^{EPv}-Gal4/UAS-GFP* mature wing discs occurs, as expected, exclusively in a central domain of the wing blade extending from the longitudinal L2 vein to the middle of the L4/L5 intervein (Figure 1, B and C). This expression is detected in the central domain of the wing disc from early L3 until 4 hr after puparium formation (not shown).

Effects on wing pattern caused by modifications in the activity of signaling pathways during imaginal development: We analyzed the range of phenotypes caused by the expression in the *spalt* domain of several proteins that either increase or reduce the activity of the Dpp, EGFR, Notch, and JNK signaling pathways. These flies were viable and fertile in all *sal^{EPv}-Gal4/ UAS* combinations tested, and the wings displayed phenotypes consistent with the known requirements of these signaling pathways (Figure 2). Thus, with activation of the Hippo pathway in the *spalt* domain, the wings are smaller and lose most structures included in this domain, such

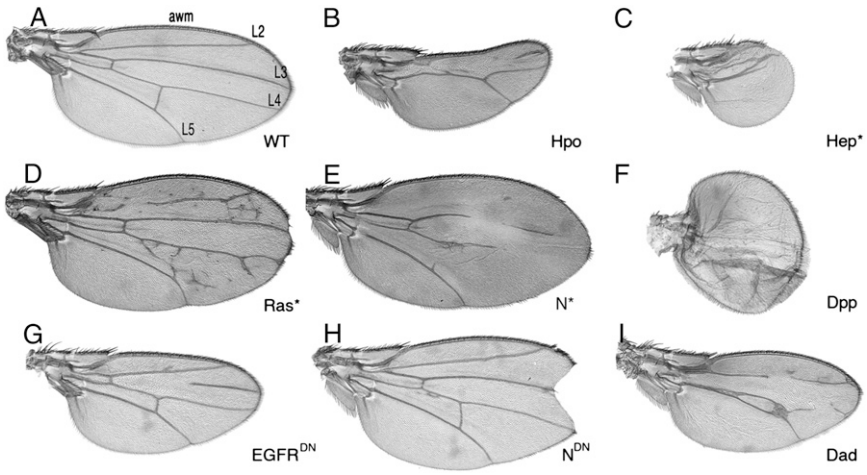

FIGURE 2.—Control wings showing the phenotype of changes in EGFR, Notch, Dpp, Hpo, and JNK signaling during imaginal development. (A) Wild-type wing (WT). The lettering indicates the longitudinal veins L2–L5 and the anterior wing margin (awm). (B–I) Wings of combinations between *sal^{EPv}-Gal4* and the UAS lines *hippo* (Hpo, B), *activated-Hemipterous* (Hep*, C), *Ras^{V12}* (Ras*, D), *N^{intra}* (N*, E), *dpp* (Dpp, F), *dominant-negative EGFR* (EGFR^{DN}, G), *dominant-negative Notch* (N^{DN}, H), and *dad* (Dad, I). Ectopic expression of *Hippo* and activated Hep reduces wing size, deleting in part (Hpo, B) or entirely (Hep*, C) the territories included in the domain of *sal^{EPv}-Gal4* expression. Loss and gain of EGFR (D and G), Notch (E and H), and Dpp (F and I) activities result in characteristic modifications in wing size, vein patterning, and wing-margin formation.

as the veins L2, L3, and L4 (Figure 2B; *sal^{EPv}-Gal4/UAS-hpo*). A more extreme phenotype, where only the region included between the L5 vein and the posterior wing margin develops, is observed when an activated version of the JNK kinase Hemipterous (Hep) is expressed in the *spalt* domain (Figure 2C; *sal^{EPv}-Gal4/UAS-hep**). Increased activity of the EGFR (*sal^{EPv}-Gal4/UAS-ras^{V12}*; Figure 2D), Notch (*sal^{EPv}-Gal4/UAS-Notch^{intra}*; Figure 2E), and Dpp pathways (*sal^{EPv}-Gal4/UAS-dpp*; Figure 2F) also modifies the size of the wing and the pattern of veins, causing the formation of ectopic veins and sensory elements (*UAS-ras^{V12}*), the loss of veins (*UAS-Notch^{intra}*), or the formation of large territories with vein characteristics in severely misshapen wings (*UAS-dpp*). The expression of modified proteins acting as dominant-negatives or antagonist of the same signaling pathways resulted in opposite phenotypes, in which the veins are lost (*sal^{EPv}-Gal4/ UAS-EGFR^{DN}*; Figure 2G and *sal^{EPv}-Gal4/ UAS-dad*; Figure 2I) or the wing margin is eliminated in its distal region (*sal^{EPv}-Gal4/UAS-Notch^{ECD}*; Figure 2H). These phenotypes are similar to those caused by loss-of-function alleles in genes belonging to the corresponding pathways, such as *vein* or *Notch* alleles (DE CELIS and GARCIA-BELLIDO 1994; GARCIA-BELLIDO *et al.* 1994) and Dpp insufficiency (MARTIN *et al.* 2004). The clear-cut phenotypes observed upon modifications of signaling in the central domain of the wing disc and the excellent viability and fertility of *trans*-heterozygous flies carrying the *sal^{EPv}-Gal4* construct and these UAS lines allowed us to use *sal^{EPv}-Gal4* to screen novel P-UAS insertions in an F_1 generation.

Phenotypic classes of novel *P-GS* in combination with *sal^{EPv}-Gal4*: We generated 3340 *P-GS* insertions by mobilizing a *P-GS* element inserted in a CyO chromosome (Figure 1A; see TOBA *et al.* 1999) and isolated as stable stocks 296 *P-GS* insertions that gave a visible phenotype in the wing in combination with *sal^{EPv}-Gal4* (Table 1). This number corresponds to a frequency of mutant phenotypes of ~9% of the tested insertions (see Figure 1A). This frequency is much higher than those observed in similar screens, which generally is 4% (see, for example, TOBA *et al.* 1999; PENA-RANGEL *et al.* 2002; MOLNAR *et al.* 2006). The high proportion of *P-GS* insertions giving wing phenotypes in combination with *sal^{EPv}-Gal4* is likely a consequence of the high viability of *sal^{EPv}-Gal4/P-GS trans*-heterozygous flies.

The phenotypes of *P-GS/sal^{EPv}-Gal4* combinations were grouped into five classes, including changes in wing **s**ize and vein **p**attern ("S-P," Figure 3A′), reductions of wing **s**ize in otherwise normally patterned wings ("S," Figure 3A′), loss or gain of longitudinal wing **v**eins ("V," Figure 3A′), failures in the formation of the **w**ing **m**argin ("WM," Figure 3A′), and a fifth class including a variety of phenotypes such as defects in epithelial integrity, cell identity, or cell differentiation ("Other," Figure 3A′). Several representative examples of wing phenotypes included in each class are shown in Figure 3, and one phenotype for each insertion site in combination with *sal^{EPv}-Gal4* or *638-Gal4* is shown in Figure S1 and Figure S2. The larger class of *P-GS* insertions (34%) include lines that, in combination with *sal^{EPv}-Gal4*, affect simultaneously the size of the wing and the pattern of veins (Figure 3, B–D, and Figure S1). In general, these phenotypes can be described as the result of a failure to develop particular wing territories with the consequent fusion of adjacent veins, mostly L2 and L3 or L4 and L5; the loss of individual veins; and the shortening of the wing blade. These phenotypes are reminiscent of those caused by inducing cell death in the *spalt* domain of expression either indirectly (through activation of the Hpo pathway) or directly (through activation of the JNK pathway) (compare Figure 2B with Figure 3C and Figure 2C with Figure 3D). In addition, reductions in Dpp activity are also expected to modify simultaneously vein formation and wing size (see Figure 2I; compare Figure 2I

TABLE 1

Insertion sites and candidate genes identified in the screen

P-GS (*n*)	Cytology	*sal-Gal4*	R	D 5′	5′ gene	MC 5′	Interactors	*n*	D 3′	3′ gene	MC 3′	Interactors	Phenotype	Pathway
s-398 (1)	1B7	S-P, CS	+	0	*CG4262 (elav)*	TF	4	2	0	*CG18104 (arg)*	M	0	N/N	CD
s-67 (1)	1E1	wt		1	*CG32814*	CGh	0	2	0	*CG3021*	RB	9	N/N	InR
s-583 (1)	2B16	S-P	+	NO				0	NO					CD
s-456 (1)	2C2	S	+	3	*CG4406*	PP	0	2	0	*CG4399 (east)*	PP	3	N/N	Dpp
s-289 (1)	3A8	S	+	10	*CG10260*	CS	0	1	0	*CG2621 (sgg)*	M	1	N/Y	Wg
s-502.2 (1)	3C7	S-Ps, CD	+	2	*CG3653 (kirre)*	CS,CA	3	2	1	*CG3936 (N)*	CS	33	Y/Y	Notch
s-445 (2)	3F1	S-Pw	+	NO				1	3	*CG34412 (tlk)*	M	0	N	Dpp
s-395 (1)	4C13	S-P, CD	+	1	*CG2984 (Pp2C1)*	CS	10	2	0	*CG6998 (ctp)*	CY	40	N/N	Dpp/[a]
s-288.1 (2)	4E2	Sw	+	3	*CG32767*	TF		1	45	*CG6775 (rg)*	CS	3	N/Y	CD
s-535 (1)	5A12	N	+	1	*CG3171 (Tre1)*	CS	1	2	1	*CG15779 (Tre)*	CS	1	Y/Y	Notch
s-281.2 (2)	5B6	S	+	0	*CG3125 (l(1)G0060)*	CA	1	2	1	*CG4078*	TF	3	N/N	Notch
s-19a (2)	5C7	V+w	+	NO				1	0	*CG4027 (Act5C)*	CY	35	N	EGFR[a]
s-163 (2)	6C7	S-Ps	+	3	*CG14440*	CGh	2	2	9	*CG14441*	TF	1	N/N	Dpp
s-562.2 (1)	6D7	S-P	+	9	*CG14434*	CGh	1	2	7	*CG33691*	CG	7	N/N	?
s-290 (4)	7A2	S-P	+	6	*CR32730*	Noncoding RNA		2	0	*CG9650*	TF	1	N/N	EGFR[a]
s-501 (2)	7B1	S	+	14	*CG1659 (unc-119)*	CS	9	1	4	*CG9653 (brk)*	TF, CS	45	N/Y	Dpp
s-378.1 (1)	7C4	S, Nw	+	1	*CG10777*	TF	4	1	NO				N	Notch
s-195 (2)	7C9	S-P	+	0	*CG2206/l(1)G1093*	CG	1	2	NO				N	CD
s-14 (1)	7F4	S-Pw	+	2	*CG12112*	CG	0	2	0	*CG11265 (Trf4-1)*	TF	20	N/N	?
s-232 (1)	8B6	S, Ew	>	0	*CG10701 (Moe)*	CY	54	1	NO				Y	?
s-407.1 (1)	8D8	S, Nw	+,E	3	*CG9060 (Zpr1)*	TF	13	2	0	*CG12218 (mei-P26)*	TF	1	N/N	Notch
s-436 (1)	8E6	S	+	1	*CG15316*	CG	1	1	NO				N	Notch
s-20 (4)	8F9	S-P	+	2/3	*CG15321/CG15319 (nej)*	CGd/TF	36	3	9	*CG12653 (btd)*	TF		N/Y/Y	Dpp
s-40 (1)	9F2	S-Pw	<	0	*CG1691 (Imp)*	RB	4	1	33	*CG15210*	RB	1	N/N	CD
s-407.2 (1)	9F5	S-P, CD	+	0	*CG1655 (sofe)*	CS	7	2	2	*CG2186*	CG	1	N/N	CC
s-147.2 (10)	13F1	S	+	2-9	*CG8995 (PGRP-LE)*	CS	4	2	0	*CG8544 (sd)*	TF	11	N/Y	CD
s-106 (1)	14A9	Sw	+, E	0	*CG42353*	CG	2	1	NO				N	InR/?
s-153.3 (3)	14B14	S-P	<	2	*CG9921*	CGh	1	2	0	*CG12223 (Dsp1)*	TF	4	N/N	CD
s-397 (1)	14C4	B	+	1	*CG9968 (Anxb11)*	CY	9	2	0	*CG32575 (hang)*	TF	3	N/N	Wg[a]/?
s-392 (1)	15A9	S	+	NO				1	0	*CG4829*	M	3	N	InR
s-401 (4)	17C3	Ns	+	NO				1	1	*CG6500 (Bx)*	TF	3	Y	Notch
s-253 (1)	18C8	S-Pw	+	0	*CG12204*	CGh	1	2	NO	*CG3400 (Pfrx)*	M	3	N/N	Dpp
s-95 (1)	18D1	S	+	0	*CG14217 (Tao-1)*	CS	4	1	NO				N	InR
s-294 (1)	18E1	S-P	<	2	*CG14229*	CGh	0	2	1	*CG12530 (Cdc42)*	CS	2	N/Y	CD
s-144 (1)	18F1	S-P	<	1	*CG12701 (vfl)*	TF	7	1	30	*CG12700 (skpD)*	M	0	Y/N	Hh/CD
s-151 (3)	18F4	V-	+	22	*CG15618*	CGh	2	1	0	*CG32529*	CGh	1	N/N	EGFR
s-409 (1)	19B3	S-P	+	3	*CG9576*	CGh	5	2	1	*CG9577*	M	5	N/N	?
s-121.2 (2)	19F6	S-Pw	<	NO				1	1	*CG1417 (slgA)*	M	19	N	Hh[a]/Moe
s-361 (1)	21B2	N, S-Pw	+	NO				1	0	*CG18497 (spen)*	CS	8	Y	Notch
s-X (1)	21F1	wt		1	*CG4644*	TF	1	2	0	*CG14339*	CGd	1	N/N	?
s-123.2 (2)	25A8	S-Pw	<	1	*CG15626*	CD	0	2	1	*CG12194*	M	2	N/N	Hh[a]/Moe
s-258 (3)	25B1	S	+	NO				0	NO					Notch[a]

(*continued*)

TABLE 1

(Continued)

P-GS (*n*)	Cytology	*sal-Gal4*	R	D 5′	5′ gene	MC 5′	Interactors	*n*	D 3′	3′ gene	MC 3′	Interactors	Phenotype	Pathway
s-154 (1)	25F1	V-	+	3	*CG10734*	CG	1	2	3	*CG8434 (lbk)*	CGh	0	N/N	?
s-529 (1)	26A1	S-P	<	3	*CG9021*	CG	1	2	0	*CG14001 (bchs)*	M	0	N/N	Hh[a]/Moe
s-527 (1)	26D8	S-P	+	2	*CG9539 (Sec61α)*	M	13	2	0	*CG9537 (DLP)*	CS	1	N/N	?
s-236 (1)	28D3	V-	+	1	*CG7233 (snoN)*	CS, TF	0	2	7	*CG7231*	CGh	20	N/N	Dpp
s-32 (1)	29A1	S-P	wt	0	*CG8049 (Btk29A)*	CS	7	1	NO				N	CD
s-138 (2)	29C3	S-P	>	0	*CG13398*	CGh	1	2	1	*CG13388 (Akap200)*	CS	3	N/N	Dpp
s-44.2 (2)	29E4	Nw, S	>	0	*CG9310 (Hnf4)*	TF	4	2	6	*CG9314*	M	0	N/N	Notch
s-183 (1)	30B12	V−, S, Nw	>	4	*CG4405 (jp)*	CGh	2	2	0	*CG3838*	TF	10	N/N	CD
s-460 (1)	30B12	S, +q	+	1	*CG12245 (gcm)*	TF	2	2	8	*CG3841*	M	0	N/N	Wg[a]
s-44.1 (1)	30C5	Ew	>	0	*CG4379 (Pka-C1)*	CS	4	3	2	*CG3949 (hoip)/ CG3959 (pelo)*	RB	7	N/N/N	Hh[a]/Moe
s-244 (1)	30C7	S-P, B	+	10	*CG4105 (Cyp4e3)*	M	0	1	0	*CG3998 (zf30C)*	TF	15	N/Y	Dpp
s-112.1 (2)	31B1	Ns	+	1	*CG5708*	TF	39	1	NO				N	Notch
s-123.1 (1)	31D11	S-P, +q	+	NO				1	0	*CG5102 (da)*	TF	18	Y	Dpp/Wg[a]
s-254 (2)	32E2	S, E	+	1	*CG6392 (cmet)*	CY	4	2	0	*CG32955 (CENP-ana)*	CY	0	Y/Y	Hh[a]/Moe
s-60 (2)	33A1	S-Pw	+	0	*CG14938 (crol)*	TF	6	1	NO				Y	Notch/Wg
s-350 (1)	34C3	S	+	0	*CG9239 (B4)*	CGh	3	1	28	*CG16852*	CG	1	Y	InR
s-161.1a (2)	35B8	V−	+	0	*CG4180 (l(2)35Bg)*	CGh	3	2	1	*CG3497 (Su(H))*	TF, CS	16	N/Y	Notch[a]/EGFR
s-132 (1)	35D1	S-Pw	<	1	*CG11861 (gft)*	PP	11	1	NO				Y	Dpp/CD
s-262 (3)	35D1	S	+; E	13	*CG15259 (nht)*	TF	0	1	1	*CG3758 (esg)*	TF	31	N/Y	InR
s-242 (1)	35F1	+qw	+	0	*CG4993 (PRL 1)*	PPh	2	2	7	*CG4930 (EndoGI)*	CGd	0	N/N	Wg[a]
s-250 (1)	35F1	S	+	0	*CG7664 (crp)*	TF	4	2	1	*CG4132 (pkaap)*	CS	0	Y/N	InR/?
s-167 (2)	36C8	N, V+	+	1	*CG6667 (dl)*	TF	52	2	2	*CG5050*	CGd	24	N/N	Notch/EGFR[a]
s-442 (1)	36D2	S	+	1	*CG15150 (elfless)*	M	23	2	1	*CG15151 (PFE)*	CS	1	N/Y	
s-563.2 (1)	38F5	S w	+	1	*CG9342 (Mtp)*	M	2	1	NO				N	InR
s-12 (2)	42C6	S-P	+	1	*CG9432 (l(2)01289)*	M	5	2	2	*CG3268 (phtf)*	TF	2	N/N	CD
s-489 (1)	43F1	S, E, ±V	[a]	1	*CG12159*	CG	1	2	0	*CG1877 (lin19)*	PP	6	N/N	Hh[a]/Moe
s-58 (1)	44A4	S-P	+	1	*CG17977*	CG	1	2	0	*CG8715 (lig)*	CGh	3	N/Y	Dpp/CD
s-37 (1)	45A8	wt		NO				1	0	*CG8068 (Su(var) 2-10)*	TF	5	N	Wg
s-532 (1)	46C2	S-P, CD	+	0	*CG1513*	M	3	2	1	*CG30007*	CG	1	N/N	Dpp/CD
s-479 (2)	46D4	V	+	1	*CG15862 (Pka-R2)*	CS	7	2	1	*CG12128*	CGh	0	Y/N	Hh[a]
s-200 (1)	46E1	S-P	<	3	*CG1371*	CGh	0	2	5	*CG12919 (egr)*	CS	4	N/Y	Dpp/CD
s-523.2 (2)	46F1	S	+	2	*CG17753 (CCS)*	M	3	2	0	*CG30011 (gem)*	TF	17	N/N	EGFR[a]
s-357 (2)	47A13	V+, S	>	48	*CG12052 (lola)*	TF	26	1	0	*CG2368 (psq)*	TF	0	N/Y	Notch
s-367 (2)	47D6	S	+	NO				1	0	*CG7734 (shn)*	TF/CS	0	Y	Dpp
s-76 (1)	48B6	V	+	0	*CG8998 (Roc2)*	M	3	2	1	*CG30035*	M	3	N/N	Dpp
s-454 (1)	49B12	S	+; E	0	*CG8776*	M	4	1	NO				N	InR
s-338 (1)	49E7	V−	+	16	*CG3886 (Psc)*	TF,M	0	1	0	*CG3905 (Su(z)2)*	TF	1	Y/Y	?
s-387 (1)	50A13	S-P, CD	+	0	*CG6033 (drk)*	CS	19	2	1	*CG17064 (mars)*	CS	6	Y/Y	CC
s-344.2 (1)	50A3	V−, E	>	NO				0	NO					Moe

(*continued*)

TABLE 1

(Continued)

P-GS (*n*)	Cytology	*sal-Gal4*	R	D 5′	5′ gene	MC 5′	Interactors	*n*	D 3′	3′ gene	MC 3′	Interactors	Phenotype	Pathway
s-563.1 (1)	50A3	Sw	+; E	9	*CG17048*	PP	1	1	NO				N	Moe
s-129 (1)	50C14	S	<	0	*CG6671 (AGO1)*	M	2	2	0	*CG30481 (mRpL53)*	CG	1	Y/Y	InR
s-380 (1)	50E1	S-P	+	0	*CG8338 (mRpS16)*	M	0	2	0	*CG8367 (cg)*	TF	10	Y/Y	Dpp/CD
s-100 (1)	50E4	S-Pw	<	0	*CG8479*	CY	7	1	NO				Y	Dpp
s-72 (1)	51A4	S-P, N	+	NO				1	1	*CG17390 (oaz)*	CGh	0	N	Dpp
s-477 (1)	52A5	Nw	+; E	7	*CG12964*	CGh	0	2	3	*CG12960 (Ir52a)*	CGh	0	N/N	Notch/EGFR
s-423.2 (1)	52D2	V−, S	+	0	*CG8291 (bdg)*	M	21	1	NO				Y	Dpp
s-35.2 (3)	53D1	Nw	<	NO				1	1	*CR33018 (mir-8)*	micro RNA		Y	Notch/EGFR
s-112.2 (3)	53E10	S-P	<	NO				1	0	*CG9635 (RhoGEF2)*	CS	3	Y	Dpp/CD
s-98 (2)	54C12	E, S	+	0	*CG6477 (RhoGAP54D)*	CS	11	2	0	*CG32031 (Argk)*	M	7		Moe
s-160 (1)	54C12	V−, S	+; E	1	*CG30105*	CGh	0	2	0	*CG4943 (lack)*	PP	1	N/Y	Dpp/Notch
s-101.1 (3)	54C3	S	+	1	*CG6510 (RpL18A)*	M	13	2	1	*CG4903 (MESR4)*	TF, CS	2	N/N	InR
s-316.1 (1)	54D3	Sw	+	12	*CG30106*	CS	1	1	0	*CG4954 (eIF3-S8)*	RB	6	N	InR
s-35.1 (3)	55B8	S-P	+	NO				1	0	*CG5119 (pAbp)*	RB	22	N	CD
s-97 (1)	55B9	S	+	0	*CG5738 (lolal)*	TF	11	2	1	*CG10914*	CGd	6	Y/N	InR
s-153.1 (2)	56D3	S-P	+	0	*CG17246 (Scs-fp)*	M	7	1	NO				N	Hh[a]/Moe
s-222.2 (1)	56E4	S	+	1	*CG9854 (hrg)*	M	1	2	0	*CG11025 (ISOT-3)*	PP	2	Y/N	Dpp
s-116 (1)	57A6	Nw, Sw	+	1	*CG13432 (l(2)05510)*	CGd	6	1	NO				N	Notch
s-339 (3)	57A6	Nw, S-Pw	+	1	*CG13434 (Nnf1a)*	CG	21	2	0	*CG13425 (bl)*	TF	2	N/Y	Notch
s-332 (1)	57B16	Ns	+	0	*CG3722 (shg)*	CS	3[a]	2	1	*CG10540 (cpa)*	CY	8	Y/Y	Notch/Wg
s-227.1 (1)	57E6	S-Pw, V-w	+	0	*CG9847 (Fkbp13)*	M	0	2	NO				N	InR
s-303 (4)	57F10	S-P	+	3	*CG30403*	CGh	2	2	0	*CG17950 (HmgD)*	TF	4	N/N	Dpp/CD
s-238 (3)	59F1	S	+	NO					0	*CG5393 (apt)*	TF	14	Y	?
s-271 (1)	60B10	S-Pw	+	0	*CG4012 (gek)*	CS	0	2	2	*CG11290 (enok)*	TF	14	N/N	?
s-69 (1)	60B4	V−, Nw	+	1	*CG3924 (Chi)*	TF	23	2	0	*CG3167 (Mam1)*	CGh	0	Y/N	Dpp/¿?
s-256 (1)	60E8	S w	+	0	*CG2790*	M	0	2	2	*CG12851*	CG	0	N/N	Notch
s-210 (2)	61C7	V+	PL					2	2/8	*ban/CG12030*	M	3	Y/N	EGFR[a]
s-108 (1)	61C8	Nw	+	0	*CG13894*	TF	1	1	NO				N	Notch
s-121.1 (2)	62A3	S	+	1	*CG12086 (cue)*	CS	0	2	0	*CG1009 (Psa)*	PP	1	N/N	InR
s-165 (1)	62B4	N	+	0	*CG1935 (JTBR)*	CGh	0	2	1	*CG12022/CG13923*	CG/CG	6/0	N/N/N	Notch
s-322 (1)	63A6	S	+	4	*CG32486*	M	13	2	0	*CG11486*	RB	61	N/N	Notch
s-118 (3)	63C1	Ew	>	5	*CG12078*	CG	0	2	9	*mir282/CG14959 (ckg)*	CG	0	N/N/N	Moe
s-186 (1)	63D1	S	+; E	1	*CG32268 (dro6)*	CGd	0	1	15	*CG12008 (kst)*	CY	6	N/Y	Notch/?
s-6 (1)	64B2	wt		0	*CG15015 (Cip4)*	CS	6	1	1	*CG15016 (mRpS6)*	RB	5	N/Y	Notch
s-274 (2)	64E5	S-P	<	1	*CG10578 (DnaJ1)*	CGd	35	2	0	*CG5486 (Ubp64E)*	PP	5	N/N	EGFR[a]/?
s-484 (1)	65A4	S-P	+	1	*CG10475 (Jon65Ai)*	M	1	2	0	*CG6586 (tan)*	TF	1	N/Y	Dpp/CD
s-156 (1)	66A19	S-P	<	1	*CG8114 (pbl)*	M	4[a]	2	0	*CG8281*	CG	2	N/N	Hh[a]/Moe
s-147.1 (1)	66A21	S	+	0	*CG8044 (HP4)*	CG	3	3	1	*CG8209/CG7892 (nemo)*	CGh/CS	0/6	N/N/Y	InR/?
s-251 (1)	66B4	S	+	3	*CR32360*	tRNA		1	NO				N	InR/?
s-481 (1)	66C8	wt		1	*CG7176 (Idh)*	M	8	1	12	*CG13668 (ImpE1)*	M	10	N/Y	
s-286 (2)	67B1	S-Pw, V−	+	NO				0	NO					EGFR
s-120 (1)	67C10	S-P, E	<	1	*CG10574 (I-2)*	PP	4	1	NO				N	CD
s-182.1 (1)	67E6	S	<	NO				1	0	*CG32067 (simj)*	TF	2	Y	Dpp

(*continued*)

TABLE 1

(Continued)

P-GS (*n*)	Cytology	*sal-Gal4*	R	D 5′	5′ gene	MC 5′	Interactors	*n*	D 3′	3′ gene	MC 3′	Interactors	Phenotype	Pathway
s-29 (1)	68A1	V+	+	0	*CG12296 (klu)*	TF	0	1	38	*CG7923 (Fad2)*	M	2	Y/N	EGFR[a]
s-66 (1)	68D2	Nw	+	NO				1	0	*CG7334 (Sug)*	M	1	N	Notch
s-382 (1)	70D7	S-P	+	1	*CG3836 (stwl)*	TF	0	2	1	*CG3919*	TF	11	N/N	CD
s-351 (1)	73D2	S-Pw	>	0	*CG9668 (Rh4)*	CS	0	2	0	*CG9949 (sina)*	PP	41	N/Y	Dpp
s-194.1 (1)	74E2	S, V+	<	0	*CG32180 (Eip74EF)*	TF	0	1	NO				Y	Hh[a]/Moe
s-83.1 (1)	75B7	S-P	>; E	0	*CG13698*	CGh	1	2	1	*CG7354 (mRpS26)*	RB	8	N/N	Dpp
s-411 (1)	75F6	V−	+	85	*CG14080 (Mkp3)*	CS,PP	0	1	6	*CG6818 (MESR6)*	CGh	0	Y/Y	EGFR
s-263.2 (1)	78A1	N	+	0	*CG10580 (fng)*	CS	1	1	NO				Y	Notch
s-171.2 (1)	79D3	Ew	+	1	*CG11523*	CG	7	2	0	*CG6395 (Csp)*	PP	4	N/N	Moe
s-276 (1)	80B2	S-P	+	0	*CG10712 (Chro)*	M	7	1	NO				N	Dpp
s-178 (3)	82D6	Ns	>; PL	0	*CG31529*	CG	0	1	NO				N	Notch/EGFR
s-Z (1)	83B7	S-P	+	2	*CG2244 (MTA1-like)*	CG	2	2	0	*CG1250 (sec23)*	CS	7	N/N	CD
s-415 (1)	85D1	S, E	+	0	*CG9755 (pum)*	RB	2	1	NO				N	Dpp/CD
s-334 (1)	85D18	V-	+	0	*CG9366 (RhoL)*	CS,CA,CY	1	2	3	*CG8149*	CD	0	N/N	Hh
s-414 (1)	85F12	S	+	0	*CG6203 (Fmr1)*	M	20	1	2	*CG3940*	M	0	N/N	Dpp
s-171.1 (1)	85F9	S	+	15	*CG5361*	PP	0	0	1	*mir317*			N/N	InR
s-562.1 (1)	86E18	S, V−	+	NO				1	0	*CG14713*	CGd	1	N	Dpp
s-329.2 (2)	86E5	N	+	22	*CG6715 (KP78a)*	CS	1	1	0	*CG17228 (pros)*	TF	7	Y	Notch/[a]
s-206 (1)	86F5	V−	+	0	*CG6923*	PP	13	1	NO				N	CD
s-149.2 (1)	86F7	S-P	*	0	*CG31364 (l(3)neo38)*	TF	6	1	NO				Y	?
s-110 (1)	87D8	S	+	NO				1	0	*CG7583 (CtBP)*	TF	45	Y	EGFR[a]
s-78 (2)	87F10	H	+	0	*CG9591 (omd)*	CGh	1	2	0	*CG9351(flfl)*	CS	2	Y/Y	Hox
s-425.1 (1)	88A3	S	+	0	*CG12537 (rdx)*	CGh	40	1	NO				Y	InR
s-143 (2)	88B1	S-P	+	0	*CG8651 (trx)*	TF	13	1	12	*CG12207*	CGh	0	Y	Hox
s-43 (3)	88E4	Nw	+	0	*CG6499*	M	0	2	2	*CG42404*	CG	6	N/N	Notch
s-185 (2)	89B9	Nw	+	45	*CG4337 (mtSSB)*	M	6	1	0	*CG6889 (tara)*	TF	1	N/Y	Notch
s-175 (1)	89D5	S		1	*CG14905*	CGh	6	2	0	*CG6588 (Fas 1)*	CA	7	N/N	InR
s-385 (1)	89E12	S	+	1	*CG3962 (Keap1)*	CY	6	2	0	*CG5175 (kuk)*	CG	5	N/N	CD
s-59.3 (1)	90C1	V+w	+	0	*CG7467 (osa)*	TF	7	2	3	*CG7660 (pxt)*	M	12	Y/N	EGFR[a]
s-518a (1)	90F11	S-Pw	+	NO				1	2	*CG18599*	CGh	0	N	Dpp
s-492 (1)	91A7	V−	+	0	*CG7688 (fru)*	TF	8	1	113	*CG7691*	CGd	1	N	Hh
s-393 (1)	91D4	S, V-w, Ew	+; E	11	*CG14291*	M	0	1	9	*CG17836*	TF	9	N/N	EGFR
s-70 (1)	92A2	B, V−	+	1	*CG3619 (Dl)*	CS	22	1	NO				Y	Notch
s-235 (3)	92F2	Nw, +q	+	1	*CG4159*	M	1	2	0	*CG5206 (bon)*	TF	1	N/Y	CD
s-408 (1)	93A1	S	+	NO				1	0	*CG33094 (Synd)*	CY	3	N	Notch/CD
s-304 (1)	93D9	S, N, E	+	9	*mod (mdg4)*	PP,TF	4	2	1	*CG7895 (tin)*	TF	1	N/N	Hh[a]/Moe
s-503 (1)	94E1	V−	+	0	*CG4637 (hh)*	CS	3	1	NO	*CG4620 (unk)*	M	1	Y/N	Hh[a]
s-85.1 (1)	94E10	S	+	0	*CG17077 (pnt)*	TF,CS	4	2	2	*CG6768 (DNApol-epsilon)*	M	1	Y/N	EGFR
s-281.1 (1)	94E9	S-P	+	0	*CG10868 (orb)*	RB	3	2	1	*CG6759 (cdc16)*	PP	3	N/N	Hh
s-439 (6)	95D10	S-P	+	0	*CG5422 (Rox8)*	RB	21	2	0	*CG5986*		0	N/N	Hox
s-455 (1)	96A9	V−, S	+	1	*CG13625*	CGh	26	2	0	*CG33343 (mld)*	CG	2	N/N	EGFR

(*continued*)

TABLE 1

(Continued)

P-GS (*n*)	Cytology	*sal-Gal4*	R	D 5′	5′ gene	MC 5′	Interactors	*n*	D 3′	3′ gene	MC 3′	Interactors	Phenotype	Pathway
s-89.1 (1)	96F10	S-Pw	+	NO				1	0	*CG8384 (gro)*	TF, CS		Y	Dpp/Wg[a]
s-422 (1)	97E10	S-P	>	0	*CG18766*	CGh	10	1	NO				N	Dpp
s-59 (9)	98A8	S-P	>	0	*CG5643 (wdb)*	PP	37	2	2	*CG5692 (raps)*	CS	35	Y/Y	EGFR/Wg
s-205.2 (2)	98F13	S	+	NO				1	0	*CG11897*	M	1	N	InR
s-349 (2)	99A1	S	+; E	2	*CG14508*	M	1	2	3	*CG31044*	CG	0	N/N	InR
s-150 (2)	100B1	S	+	1	*CG1715 (l(3)03670)*	CGh	0	1	NO				Y	Dpp
s-127 (5)	100D1	S-P	<	45	*CG11550*	M	0	1	0	*CG11558 (ttk)*	TF	39	Y	CD
s-423.1 (1)	102C2	S-P	+	14	*CG11533 (CKI-like)*	CS	2	0	19	*CG1449 (zfh2)*	TF	2	Y	CD

Each insertion site is represented by one *P-GS* line, and the number of insertions in the same genomic location is indicated within parentheses. Data are ordered by cytological position. Phenotypes in combination with *sal^{EPv}-Gal4 (sal-Gal4)* are the following: effects on wing size and vein pattern (S-P), reduction of wing size (S), loss of veins (V−), defects in cell differentiation (CD), fails in dorso-ventral adhesion (B), defects in wing folding (F), formation of wing-margin nicks (N), defects in epithelial integrity (E), and wild type (wt). The "w" and "s" indicate a "weak" or "strong" phenotype, respectively, compared to others in the same phenotypic class. The "R" column indicates the result of the *P-GS/ sal^{EPv}-Gal4; UAS-puc/+* combination. "+" indicates no phenotypic effect, ">" indicates enhancement, and "<" suppression of the *P-GS/ sal^{EPv}-Gal4* phenotype by Puc. "E" indicates the presence of cuticle differentiated between the dorsal and ventral wing surfaces. D 5′ and D 3′ indicate the distance in kilobases from the insertion site to the 5′-end of the genes located proximally (D 5′) and distally (D 3′). NO (not oriented) indicates a gene located within 10 kb of the insertion site but oriented with its 3′-end closer to this site than its 5′-end. "5′ gene" and "3′ gene" refer to the name of the genes located proximal (5′ gene) and distal (3′ gene) in the chromosome to the corresponding insertion site. MC 5′ and MC 3′ represents the **m**olecular **c**lass of the gene corresponding to the following: cell signaling (CS); transcription factor (TF); cell adhesion (CA); cytoskeleton (CY); metabolism (M); proteases (PP); RNA binding (RB); annotated genes with unknown function without homology (CG), with homology (CGh), and with conserved structural domains (CGd). "Interactors" refers to the number of interactors detected by two-hybrid experiments, as annotated in the BioGrid database (http://www.thebiogrid.org/), for each candidate gene. The "Phenotype" column represents the exsistence of a previous assignation (Y for positive and N for negative) of a phenotype in the wing for each candidate gene (FlyBase). The "Pathway" column indicates the similarity of the overexpression phenotypes to specific pathways. CD, cell death; CC, cell cycle; InR, insulin receptor pathway; Dpp, Decapentaplegic pathway; Wg, wingless pathway; Hh^a/Moe, changes in Hedgehog signaling associated with epithelial defects typical of *moesin* alleles (Molnar and de Celis 2006. ?, unassigned; PL, pupal lethality; H, haltere tissue; +q, extra chaetae.

[a] The phenotype of overexpression corresponds to the activation of the pathway.

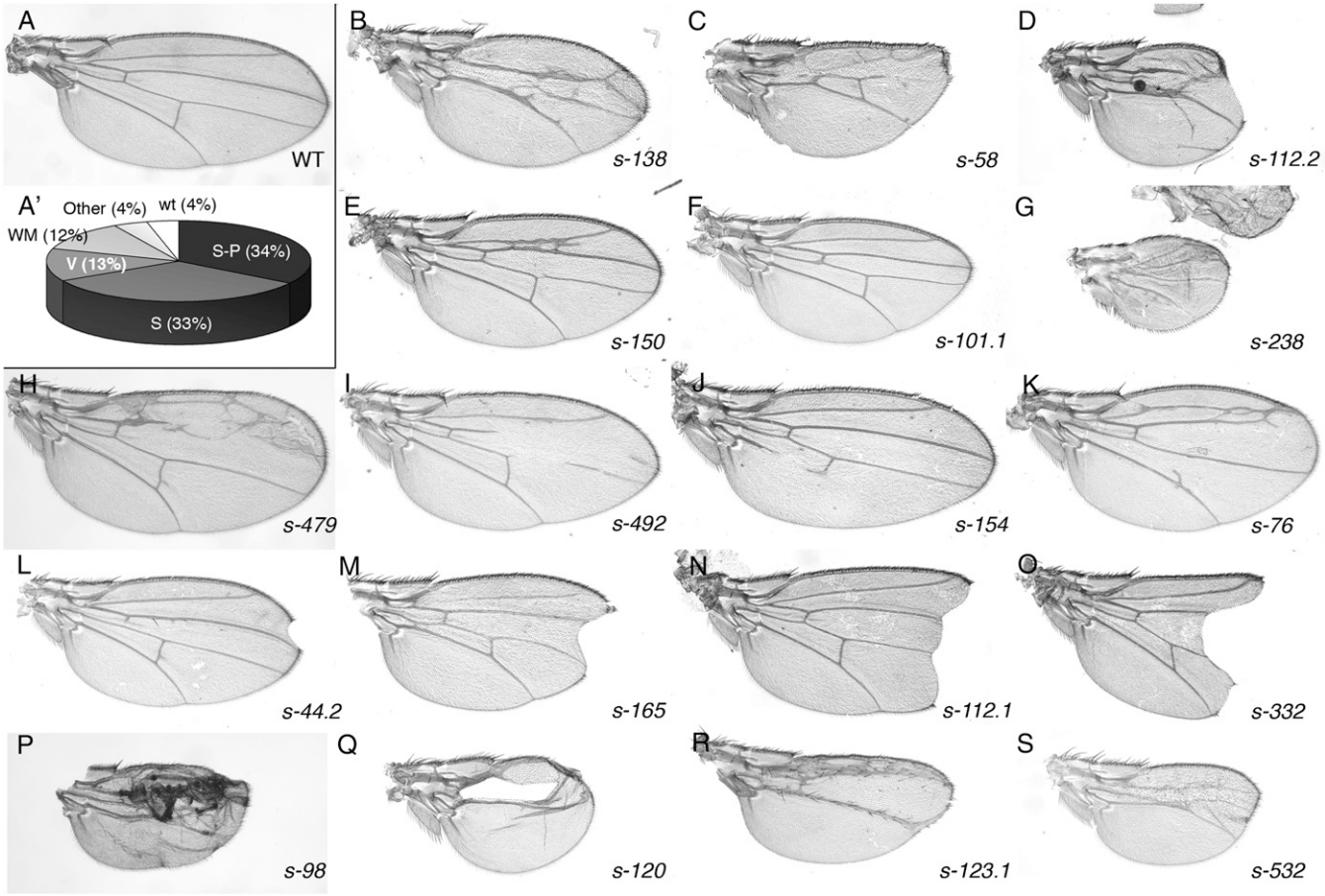

FIGURE 3.—Frequencies and examples of the phenotypic classes identified in the screen. (A) Wild-type wing. (A′) Phenotypic classes of *P-GS/sal*^{EPv}*-Gal4* combinations. Insertion sites were grouped in six phenotypic classes, and the fraction of sites belonging to each class is expressed as a percentage of the total number of insertion sites. Thirty-four percent of insertion sites result in defects in the size and pattern of the wing (S-P), 33% produce wings of smaller size with an almost normal pattern of vein, 13% affect mostly vein formation (V), 12% disrupt the wing margin (WM), and 4% affect other aspects of the wing such as cell identity or trichome differentiation. (B–D) Representative examples of *sal*^{EPv}*-Gal4/P-GS* wings where both the size of the wing and the pattern of veins are affected. (E–G) Representative examples of *sal*^{EPv}*-Gal4/P-GS* wings where mainly the size of the wing is affected. (H–K) Representative examples of *sal*^{EPv}*-Gal4/P-GS* wings where mainly the pattern of veins is disrupted. (L–O) Representative examples of *sal*^{EPv}*-Gal4/P-GS* wings where mainly the integrity of the wing margin is lost to different degrees. (P–S) Representative examples of *sal*^{EPv}*-Gal4/P-GS* wings belonging to the phenotypic class "others." In these wings, epithelial integrity is disrupted (P and Q), ectopic sensory organs differentiate along the remnants of vein tissue (R), and cells in the *sal*^{EPv} domain of expression are larger than normal and differentiate multiple trichomes (S).

and Figure 3, B and C). The second phenotypic class includes *P-GS* insertions that modify the size of the wing without causing major effects in the patterning or differentiation of the veins (Figure 3, E–G, and Figure S2). Individual *P-GS* insertions cause different degrees of wing-size reduction, and, although we did not systematically analyze whether modifications in cell size or number were responsible for the wing-size reductions, in the cases studied (four), both cell size (trichome density) and number were affected in different degrees. Wing-size reductions without significant effects on pattern are characteristic of reductions in TGFβ and insulin signaling (BRUMMEL *et al.* 1999b; BROGIOLO *et al.* 2001). A third phenotypic class including ~13% of the isolated *P-GS* insertions is characterized by defects in vein patterning without drastic changes in wing size (Figure 3, H–K). Most commonly, vein patterning is affected by the loss of individual longitudinal veins (Figure 3, H–J, and Figure S1), but in a number of cases the veins differentiate along their entire length, and only the distance between adjacent veins is altered, resulting in the change of the size of the corresponding intervein region (Figure 3K). In most cases, loss of vein tissue is restricted to the veins included in the domain of *sal*^{EPv} expression (L2–L4), but in one exceptional case, only the L5 vein is lost (Figure 3J), indicating a nonautonomous effect of the overexpressed gene. *P-GS* lines that, in combination with *sal*^{EPv}*-Gal4* interfere with vein differentiation, are candidates for identifying genes involved in the signaling pathways controlling vein formation, such as EGFR or Notch (DE CELIS 1998) (see Figure 2), whereas changes in the

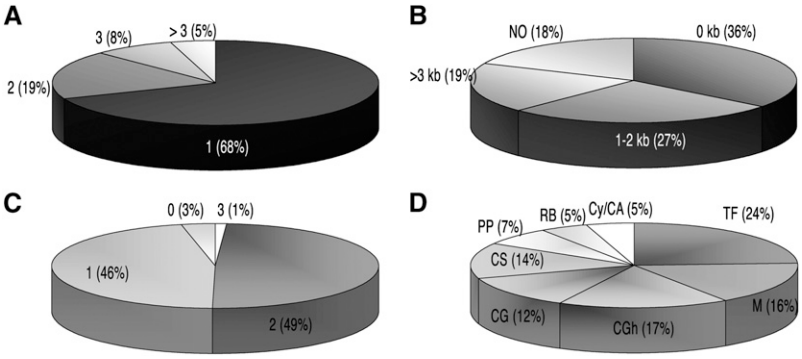

FIGURE 4.—Numerical parameters of the screen. (A) Fraction of insertion sites with one (black), two (dark gray), three (light gray), and more than three (white) *P-GS* insertions. Most genomic sites have been identified by only one insertion (68%). (B) Grouping of *P-GS* insertions by the distance in kilobases of the insertion site to the closest adjacent gene. Most of the insertions are situated within a gene or at a distance of <2 kb (63%). (C) Number of candidate genes by insertion site. Most insertion sites have one (46%) or two (49%) candidate genes. (D) Grouping of candidate genes in molecular classes following their GO annotations. TF (24%): proteins involved in transcriptional regulation; M (16%): proteins involved in cellular metabolism; CGh (17%): predicted coding sequences bearing annotated structural domains; CG (12%): predicted coding sequences for which there is no informative GO annotation; CS (14%): proteins involved in cell signaling; PP (7%): proteins with a protease domain; RB (5%): ribosomal proteins; Cy/CA (5%): proteins involved in cell adhesion or cytoskeleton dynamics.

distance between adjacent veins are generally associated with modifications in Dpp or Hedgehog signaling.

The fourth phenotypic class includes all *P-GS* insertions, the major effect of which is the loss of distal wing structures (12%; Figure 3, L–O, and Figure S2). The extent of wing-tissue loss is characteristic of each individual *P-GS* line, and this phenotype suggests a failure in the formation or maintenance of the dorsoventral boundary, a process in which signaling by the Notch- and Wg-signaling pathways plays a prominent role (IRVINE and VOGT 1997) (see Figure 2H). Finally, a number of *P-GS* insertions, in combination with *sal^{EPv}-Gal4*, gave phenotypes that could not be easily classified in the preceding classes (Figure 3, P–S, and Figure S2). Several examples of these phenotypes are defects in epithelial integrity (Figure 3P), holes in the center of the wing (Figure 3Q), fusion of veins and formation of ectopic sensilla (Figure 3R), and defects in trichome formation, such as the differentiation of several trichomes by each wing cell in the central region of the wing (Figure 3S).

Distribution of *P-GS* insertion sites: The insertion site of 296 *P-GS* lines was identified following a protocol of inverse PCR, sequencing, and nBlast (see MATERIALS AND METHODS and Table S1). These data are summarized in Table 1, which also indicates the cytological position of each insertion, the number of insertions isolated in each genomic site, and the proximal (5′) and distal (3′) genes adjacent to the insertion sites. Most insertion sites (68%) were targeted by only one *P-GS* element, indicating that the screen is far from saturation (Figure 4A). Sites with more than three insertions (5%) correspond to previously identified "hot spots" (SPRADLING *et al.* 1995). The distribution of novel insertions with respect to the 5′-end of the adjacent transcripts also follows the known pattern of *P* elements (LIAO *et al.* 2000), and most insertions (63%) are within 2 kb of the 5′-end of the affected transcription unit (Figure 4B). The *P-GS* element carries two sets of UAS sequences located at its ends, and therefore the genes located both proximal and distal to the insertion site are expressed under the control of these sequences (MOLNAR *et al.* 2006). In this manner, the identification of the insertion site allows only the determination of the gene or genes candidate that causes the gain-of-function phenotype. Using the criteria determined in a previous *P-GS* screen (MOLNAR *et al.* 2006), we annotated as candidate genes that cause the overexpression phenotype all coding sequences in which both the 5′-end is located <10 kb from the insertion site and closer to this site than the corresponding 3′-end. A large fraction of *P-GS* insertion sites (49%; Figure 4C) have two candidate genes, very few have more than two or no candidate genes (3% in each class; Figure 4C), and the remaining insertion sites have only one candidate gene (46%; Figure 4C). From previous experience we also know that most mutant phenotypes are caused by the expression of only one gene, and in this manner the number of 260 candidate genes identified in the screen corresponds to an overestimation of the genes actually responsible for the gain-of-function phenotypes.

The 260 candidate genes identified fall into several molecular classes, among which the more abundant correspond to genes encoding transcription factors and other proteins involved in the regulation of gene expression (24%; TF in Figure 4D). Another group is composed of annotated genes without clear homologs and with no functional Gene Ontology (GO) annotation (29%, CG and CGh in Figure 4D). More than half the genes included in this class, however, encode proteins with a variety of conserved structural domains (17%, CGh in Figure 4D). Other molecular or functional categories represented in the screen are genes involved in cell signaling (14%, CS in Figure 4D), protein phosphatases (7%, PP in Figure 4D) and proteins that are likely to regulate cell adhesion and cytoskeleton dynamics (5%, Cy/CA in Figure 4D). Among the candidate genes identified are 24 known members of the signaling pathways that regulate wing formation, 21 genes that encode transcription factors

TABLE 2

Phenotype of *P-GS* insertions in combination with *638-Gal4*, *shv-Gal4*, *253-Gal4*, and *ey-Gal4*

P-GS	Cytology	*638-Gal4*	*shv-Gal4*	*253-Gal4*	*ey-Gal4*	Gen 5′	Gen 3′
				Size and pattern (*P-GS/sal^{EPv}-Gal4*)			
s-149.2	86F7	F	S, CD, B	wt	2	*CG31364* [*l(3)neo38*i]	
s-143	88B1	H	wt	wt	3-ne	*CG8651 (trx)*	*CG12207*
s-59	98A8	H	S, CD, B	QD	2	*CG5643 (wdb)*	*CG5692 (raps)*
s-127	100D1	L	L	wt	3	*CG11550*	*CG11558 (ttk)*
s-423.1	102C2	L	CD	No Mq	3	*CG11533 (CKI-like)*	*CG1449 (zfh2)*
s-153.3	14B14	L	B, L	wt		*CG9921*	*CG12223 (Dsp1)*
s-556	18C7	L	L	No Mq, −Sct	3	*CG14199/CG12204*	*CG3400 (Pfrx)*
s-253	18C8	L	L	−Mq	3, L	*CG12204*	
s-294	18E1	L	F, CD	−Mq, S	L	*CG14229*	*CG12530 (Cdc42)*
s-144	18F1	L	L	−Mq, S	3	*CG12701*	*CG12700 (skpD)*
s-409	19B3	L	L	−Mq, −Sct	3, L	*CG9576*	*CG9577*
s-121.2	19F6	L	CD	S	2		*CG1417 (slgA)*
s-529	26A1	L	F	−Mq	3, L	*CG9021*	*CG14001 (Beach1)*
s-527	26D8	L	F	S	3-nh, L	*CG9539 (Sec61α)*	*CG9537 (DLP)*
s-583	2B16	L	L	−Mq, L			
s-244	30C7	L	F	S	2	*CG4105 (Cyp4e3)*	*CG3998 (zf30C)*
s-132	35D1	L	CD	wt	1	*CG11861 (gft)*	
s-445	3E8	L	L	wt	1		*CG32782 (tlk)*
s-12	42C6	L	wt	−Mq, L	3, L	*CG9432* [*l(2)01289*]	*CG3268 (phtf)*
s-380	50E1	L	L	−Mq		*CG8338 (mRpS16)*	*CG8367 (cg)*
s-100	50E4	L	wt	+Mq	2	*CG8479*	
s-72	51A4	L	CD, Bs	−Mq, L	L		*CG17390*
s-112.2	53E10	L	B, CD, S	−Mq	3		*CG9635 (RhoGEF2)*
s-35.1	55B8	L	L	−Mq	2		*CG5119 (pAbp)*
s-303	57F10	L	L	−Mq, L	L	*CG30403*	*CG17950 (HmgD)*
s-274	64E5	L	CD	wt	3, L	*CG10578 (DnaJ1)*	*CG5486 (Ubp64E)*
s-156	66A19	L	B	±Mq, L		*CG8114 (pbl)*	*CG8281*
s-562.2	6D7	L	L	−Mq	1	*CG14434*	*CG32737*
s-382	70D7	L	L	−Mq	L	*CG3836 (stwl)*	*CG3919*
s-351	73D2	L	L	−Mq	3, L	*CG9668 (Rh4)*	*CG9949 (sina)*
s-290	7A2	L	L	±Mq, L	2, L	*CR32730*	*CG9650*
s-195	7C9	L	L	L	L	*CG2206*	*CG1531*
s-14	7F4	L	L		L	*CG12112*	*CG11265*
s-276	80B2	L	L	QD	2	*CG10712 (Chro)*	
s-Z	83B7	L	L	L	L	*CG31545*	*CG1250 (sec23)*
s-20	8F9	L	L	L	2–3, L	*CG15321/CG15319 (nej)*	*CG12653 (btd)*
s-281.1	94E9	L	CD			*CG10868 (orb)*	*CG6759 (cdc16)*
s-89.1	96F10	L	F	−Mq	3		*CG8384 (gro)*
s-422	97E10	L	CD	−Mq	3, L	*CG18766*	
s-398	1B7	Ns	F, B	−Mq	3, L	*CG4262 (elav)*	*CG18104 (arg)*
s-32	29A1	Ns	V+	±Mq	3	*CG8049 (Btk29A)*	
s-60	33A1	Ns	S, CD, B	wt	1	*CG14938 (crol)*	
s-58	44A4	Ns	F, L	QD	2	*CG17977*	*CG8715 (lig)*
s-387	50A13	Ns	CD	−Mq	3	*CG6033 (drk)*	*CG17064 (gkap)*
s-227.1	57E6	Ns	wt	wt	2	*CG9847 (Fkbp13)*	*CG10496*
s-271	60B10	Ns	L	−Mq, QD	3	*CG4012 (gek)*	*CG11290 (enok)*
s-83.1	75B7	Ns	CD	wt	2	*CG13698*	*CG7354 (mRpS26)*
s-439	95D10	Ns	B	−Mq	2	*CG5422 (Rox8)*	*CG5986*
s-40	9F2	Ns	CD	wt	2	*Cg1691 (Imp)*	*CG15210*
s-407.2	9F5	Ns	CD	−Mq	3	*CG1655 (sofe)*	*CG2186*
s-286	67B1	Ns, CD	V−	−Mq	3		
s-138	29C3	Ns, E	F	−Mq	3	*CG13398*	*CG13388 (Akap200)*
s-163	6C7	Ns, V−	L	wt	2	*CG14440*	*CG14441*
s-123.2	25A8	nW	CD	wt	1	*CG15626*	*CG12194*
s-502.2	3C7	Nw	wt	−Mq	2	*CG3653 (kirre)*	*CG3936 (N)*
s-532	46C2	nW	wt	wt	3, L	*CG1513*	*CG30007*
s-200	46E1	nW	F	L	1	*CG1371*	*CG12919 (eiger)*

(*continued*)

TABLE 2

(Continued)

P-GS	Cytology	*638-Gal4*	*shv-Gal4*	*253-Gal4*	*ey-Gal4*	Gen 5′	Gen 3′
s-120	67C10	nW	F	−Mq	3, L	*CG10574 (I-2)*	
s-123.1	31D11	V+	L	L	wt		*CG5102 (da)*
s-395	4C13		L			*CG2984 (Pp2C1)*	*CG6998 (ctp)*
				Size (*P-GS/sal^{EPv}-Gal4*)			
s-232	8B6	B	CD	wt	1	*CG10701 (Moe)*	
s-182.1	67E6	B, V−, Nw	B	−Mq	1		*CG32067 (simj)*
s-563.1	50A3	F	wt	wt	1	*CG17048*	
s-262	35D1	F, CD	F, CD	−Mq	1–2	*CG15259 (nht)*	*CG3758 (esg)*
s-523.2	46F1	H	L	−Mq	wt	*CG17753 (CCS)*	*CG30011 (gem)*
s-456	2C2	L	F	QD	L	*CG4406*	*CG4399 (east)*
s-442	36D2	L	L	−Mq, L	2	*CG15150 (elfless)*	*CG15151 (PFE)*
s-153.1	56D3	L	wt	wt	2	*CG17246 (Scs-fp)*	
s-251	66B4	L	CD	−Mq	L	*CR32360*	
s-414	85F12	L	L	wt	3, L	*CG6203 (Fmr1)*	*CG3940*
s-171.1	85F9	L	B, V−	QD	2	*CG5361*	
s-518a	90F11	L	CD	−Mq	3, L		*CG18599*
s-85.1	94E10	L	V−	−Mq	1	*CG17077 (pnt)*	*CG6768 (DNApol-ε)*
s-349	99A1	L	B	wt, L	1–2	*CG14508*	*CG31044*
s-254	32E2	L	F, CD	−Mq	2	*CG6392 (cmet)*	*CG32955 (CENP-ana)*
s-415	85D1	L	F	−Mq	2, L	*CG9755 (pum)*	
s-489	43F1	L	L	−Mq	2	*CG12159*	*CG1877 (lin19)*
s-304	93D9	L	L	L	3, L	*mod (mdg4)*	*CG7895 (tin)*
s-194.1	74E2	L	L	+Mq, L	2	*CG2180 (Eip74EF)*	
s-289	3A8	N	wt	wt	2	*CG10260*	*CG2621 (sgg)*
s-101.1	54C3	N	wt	wt	2	*CG6510 (RpL18A)*	*CG4903 (MESR4)*
s-256	60E8	N	F	−Mq, QD	1	*CG2790*	*CG12851*
s-186	63D1	N, CD	wt	−Mq	2	*CG32268 (dro6)*	*CG12008 (kst)*
s-322	63A6	N, V−	wt	wt	1	*CG32486*	*CG11486*
s-450	13F1	Ns	F	QD	2–3	*CG8995 (PGRP-LE)*	*CG8509*
s-436	8E6	Ns	CD	wt	1	*CG15316*	
s-408	93A1	Ns	CD	QD	2-nh		*CG15694 (Synd)*
s-175	89D5	Ns	F, B			*CG14905*	*CG6588 (Fas 1)*
s-378.1	7C4	Ns	L	wt	1–2	*CG10777*	
s-407.1	8D8	Ns	CD	QD	2	*CG9060 (Zpr1)*	*CG12218 (mei-P26)*
s-393	91D4	Ns, L	F	−Mq	2	*CG14291*	*CG17836*
s-250	35F1	Ns, V−	V−	−Mq	1	*CG7664 (crp)*	*CG4132 (pkaap)*
s-367	47D6	nW	F, V+	−Mq	3, L		*CG7734 (shn)*
s-129	50C14	nW	N, CD	−Mq	1	*CG6671 (AGO1)*	*CG30481 (mRpL53)*
s-222.2	56E4	nW	CD	−Mq	3	*CG9854 (hrg)*	*CG11025 (ISOT-3)*
s-288.1	4E2	nW	L	−Mq, QD	2	*CG32767*	*CG6789*
s-385	89E12	nW, L	wt	−Mq, QD	3	*CG3962 (Keap1)*	*CG5175 (kuk)*
s-205.2	98F13	nW, L	CD	wt	2		*CG11897*
s-562.1	86E18	Nw, V−	wt	wt	1		*CG14713*
s-392	15A9	S	wt	wt	1–2		*CG4829*
s-95	18D1	S	wt	+Mq	2	*CG14217 (Tao-1)*	
s-121.1	62A3	S	F	QD	1	*CG12086 (cue)*	*CG1009 (Psa)*
s-425.1	88A3	S	L	wt	wt	*CG9924*	
s-106	14A9	B	F	wt	wt	*CG9216*	
s-563.2	38F5	S	wt	−Mq	wt	*CG9342*	
s-460	30B12	S, +q	L	+Mq	2	*CG12245 (gcm)*	*CG3841*
s-110	87D8	S, V+	CD	−Mq	2		*CG7583 (CtBP)*
s-258	25B1	S,V−	wt	wt	wt		
s-350	34C3	Ss	wt	QD	2	*CG9239 (B4)*	*CG16852*
s-97	55B9	Ss	wt	QD	wt	*CG5738 (lolal)*	*CG10914*
s-238	59F1	Ss	L	QD	1		*CG5393 (apt)*
s-501	7B1	Ss, V−	V−	wt	1	*CG1659 (unc-119)*	*CG9653 (brk)*
s-281.2	5B6	Sw, Nw	wt	wt	1–2	*CG3125 [l(1)G0060]*	*CG4078*
s-147.1	66A21	Sw, Nw, CD	B, CD	±Mq	wt	*CG8044*	*CG8209*

(*continued*)

TABLE 2

(Continued)

P-GS	Cytology	*638-Gal4*	*shv-Gal4*	*253-Gal4*	*ey-Gal4*	Gen 5′	Gen 3′
s-316.1	54D3	wt	wt	wt	wt	*CG30106*	*CG4954 (eIF3-S8)*
				Vein pattern (*P-GS/sal^{EPv}-Gal4*)			
s-411	75F6	H	V−	wt	3	*CG14080 (Mkp3)*	*CG6818 (MESR6)*
s-161.1a	35B8	L	V−	−Mq	1	*CG4180* [*l(2)35Bg*]	*CG3497*[*Su(H)*]
s-334	85D18	L	wt	−Mq		*CG9366 (RhoL)*	*CG8149*
s-492	91A7	L	L	−Mq	2	*CG7688 (fru)*	*CG7691*
s-210	61C7	L	L	+Mq, L	L	*CG32345*	*CG12030*
s-29	68A1	L	F, CD	QD	wt	*CG12296 (klu)*	*CG7923 (Fad2)*
s-357	47A13	L	L	QD	1	*CG12052 (lola)*	*CG2368 (psq)*
s-19a	5C7	N	wt	−Mq	1–2		*CG4027 (Act5C)*
s-344.2	50A3	N, B, L	F	wt	1–2		
s-338	49E7	N, S-P	wt	−Mq	1	*CG3886 (Psc)*	*CG3905* [*Su(z)2*]
s-455	96A9	N, V−	V−	+Mq	2-L	*CG13625*	*CG33343*
s-206	86F5	N, V+	B	wt	wt	*CG6923*	
s-69	60B4	Ns	V−	±Mq	1–2	*CG3924 (Chi)*	*CG3167*
s-160	54C12	Ns	V+	−Mq	2	*CG30105*	*CG4943 (lack)*
s-183	30B12	Ns, +Mq	CD	+Mq	2	*CG4405 (jp)*	*CG3838*
s-151	18F4	V−	wt	−Mq	wt	*CG15618*	*CG32529*
s-154	25F1	V−	wt	wt	wt	*CG10734*	*CG8434 (lbk)*
s-503	94E1	V−	wt	wt	wt	*CG4637 (hh)*	*CG4620 (unk)*
s-423.2	52D2	V+	V−	wt	wt	*CG8291*	
s-59.3	90C1	V+	V+	wt	2	*CG7467 (osa)*	*CG7660 (pxt)*
s-236	28D3	V+w	V−, S	wt	wt	*CG7233 (snoN)*	*CG7231*
				Wing margin (*P-GS/sal^{EPv}-Gal4*)			
s-185	89B9	F, V+	CD	QD, L	1-L	*CG4337 (mtSSB)*	*CG6889 (tara)*
s-332	57B16	H	wt	−Mq	nh, L	*CG3722 (shg)*	*CG10540*
s-165	62B4	L	L	−Mq, S	3, L	*CG1935 (JTBR)*	*CG32317*
s-329.2	86E5	L	F, N	−Mq, S	2-L	*CG6715 (KP78a)*	*CG17228 (pros)*
s-361	21B2	L	CD,F	+Mq	2–3		*CG18497 (spen)*
s-167	36C8	L	V+	±Mq	3	*CG6667 (dl)*	*CG5050*
s-178	82D6	L	L	QD	3	*CG31529*	
s-108	61C8	N	wt	−Mq	wt	*CG13894*	
s-477	52A5	N, V−	wt	wt	3	*CG12964*	*CG12960*
s-35.2	53D1	N, V−	CD	wt	3		*CR33018 (mir-8)*
s-235	92F2	N, V−	CD	wt	wt	*CG4159*	*CG5206 (bon)*
s-112.1	31B1	Ns	wt	wt	wt	*CG5708*	
s-484	65A4	Ns	Ns	−Mq	2	*CG10475 (Jon65Ai)*	*CG6586 (tan)*
s-43	88E4	Ns	N	+Mq	1	*CG6499*	*CG4285*
s-66	68D2	Ns	wt	wt	2–3		*CG7334 (Sug)*
s-401	17C3	nW		wt	wt		*CG600 (Bx)*
s-44.2	29E4	Nw	F, CD	+Mq	1–2	*CG9310 (Hnf4)*	*CG9314*
s-116	57A6	Nw, V+	wt	wt	1	*CG13432 (l(2)05510)*	
s-339	57A6	V+w	wt	wt	1	*CG13434*	*CG13425 (bl)*
				Other (*P-GS/sal^{EPv}-Gal4*)			
s-44.1	30C5	B, Nw	B, F	wt	L	*CG4379 (Pka-C1)*	*CG3949 (hoip)*
s-78	87F10	H	wt	wt	wt	*CG9591*	*CG9351(flfl)*
s-242	35F1	L	V−	−Mq	wt	*CG4993 (PRL 1)*	*CG4930*
s-70	92A2	L	V+	wt	wt	*CG3619 (Dl)*	
s-171.2	79D3	L	F	−Mq	3	*CG11523*	*CG6395 (Csp)*
s-X	21F1	L	wt	wt	1–2	*CG4644*	*CG14339*
s-231	3E5	L	L	L	L	*CG2849 (Rala)*	*CG12462*
s-6	64B2	N	CD	QD	1	*CG15015 (Cip4)*	*CG15016 (mRpS6)*
s-98	54C12	N, CD	CD	−Mq	2	*CG6477 (RhoGAP54D)*	*CG4929 (icln)*
s-37	45A8	Nw	CD	wt	2–3		*CG8068* [*Su(var)2-10*]
s-397	14C4	S, +q	V−	wt	wt	*CG9968 (Anxb11)*	*CG32575 (hang)*

(*continued*)

TABLE 2

(Continued)

P-GS	Cytology	*638-Gal4*	*shv-Gal4*	*253-Gal4*	*ey-Gal4*	Gen 5′	Gen 3′
s-67	1E1	S, V−	CD	wt	wt	*CG32814*	*CG3021*
s-454	49B12	S, V±	F	+Mq	1	*CG8776*	
s-118	63C1	S, V-w	wt	+Mq	wt	*CG12078*	*CG14959*
s-481	66C8	wt	wt	wt	wt	*CG7176 (Idh)*	*CG13668 (ImpE1)*

Insertion sites were grouped in phenotypic classes following the *P-GS/sal^{EPv}-Gal4* phenotype. The phenotype of the combination of each *P-GS* with *638-Gal4*, *shv-Gal4*, *253-Gal4*, and *ey-Gal4* is shown. Phenotypes observed with *638-Gal4* (*638-Gal4* column head) are lethality (L), thicker veins (V+), loss of veins (V−), loss of wing margin (N), strong loss of wing margin (Ns), reduced wing size (S), reduced wing size with defects in vein patterning (S-P), defects in dorso-ventral adhesion (B), defects in wing expansion (F), defects in epithelial integrity (E), halter formation (H), loss of wing (nW), extra bristles (+q), and wild type (wt). Phenotypes observed with *shv-Gal4* (*shv-Gal4* column head) also include defects in cell differentiation (CD). Phenotypes observed with *253-Gal4* (*253-Gal4* column head) are extra bristles (+Mq), loss of bristles (−Mq), incorrect bristle differentiation or size (QD), loss of scutellum (Sct), and wild type (wt). Phenotypes observed in combination with *ey-Gal4* (*ey-Gal4* column head) consisted of reductions in eye size and were grouped in classes described as weak (1), moderate (2), and strong (3). "nh" indicates loss of the head.

previously known to participate in wing patterning, and 8 genes that regulate epithelial development (Table S2), validating the gain-of-function approach to identifying genes required for wing development.

Phenotypic specificity of novel *P-GS* insertions: All *P-GS* insertions were identified in combination with *Gal4-sal^{EPv}*, which drives Gal4 expression during the third larval instar in a central region of the wing blade. To analyze whether these lines also affected other wing regions, imaginal tissues, and developmental processes, we crossed a majority of the *P-GS* insertions with Gal4 lines expressed in the entire wing blade (*638-Gal4*), the developing pupal veins (*shv-Gal4*), the sensory organs (*253-Gal4*), and the eye region of the eye-antenna imaginal disc anterior to the morphogenetic furrow (*ey-Gal4*). As expected, all *P-GS* insertions gave a mutant phenotype in combination with *638-Gal4*, although a considerable fraction of these combinations (39%) were lethal (Table 2). The phenotype of the viable combinations fell into the same phenotypic classes identified in the screen, including those affecting the wing margin (Figure 5, B–D), modifying wing size by either reducing it (Figure 5, E–G) or increasing it (Figure 5H), eliminating the longitudinal veins (Figure 5, I–L) with (Figure 5I and L) or without (Figure 5, J and K) effects on the formation of the wing margin, and causing the formation of extra vein tissue (Figure 5, M and N). Other phenotypes observed in combination with *638-Gal4* included homeotic transformations (Figure 5, O and P), folded wings (Figure 5Q), ectopic sensory organs in the wing blade (Figure 5R), trichome morphology (Figure 5S), and wing-to-notum transformations (Figure 5, H and T).

Similarly, a large fraction of *P-GS* combinations with other Gal4 drivers also resulted in mutant phenotypes (83% with *ey-Gal4*, 77% with *shv-Gal4*, and 66% with *253-Gal4*), indicating that there is no strong tissue- or developmental-time-specific effects of the overexpressed genes. The phenotypes most frequently observed were lethality and size and pattern effects in combination with *638-Gal4* (39% and 36%, respectively); lethality and wings unfolded or failures in dorso-ventral adhesion in combination with *shv-Gal4* (24% and 22%, respectively); and different degrees of reduction in eye size in combination with *ey-Gal4* (76%, of which 30% correspond to moderate reduction and 23% to weak and strong reductions). The combinations with *253-Gal4* affected the formation of bristles, causing the duplication of macrochaetae (Figure 6A), the formation of clusters of macrochaetae in each position (Figure 6B), the loss of macro and microchaetae (Figure 6, C and D), and defects in chaetae differentiation such as the loss of the tricogen accompanied by a duplication of the tormogen (Figure 6E). The most frequent phenotypes in the combinations with *253-Gal4* were loss of chaetae and failures in chaetae differentiation (39% and 12%, respectively). The *P-GS* insertions that, in combination with *sal^{EPv}-Gal4*, affected size and pattern gave stronger phenotypes with higher frequency when combined with the other Gal4 drivers. For example, 60% and 40% of these lines were lethal in combination with *638-Gal4* and *shv-Gal4*, respectively, 43% of these lines gave strong eye phenotypes in combination with *ey-Gal4*, and 50% of these lines resulted in loss of bristles in combination with *253-Gal4*. In general, there was consistency between the wing phenotypes of combinations involving different drivers expressed in the wing and a given *P-GS* insertion. Several examples of the phenotypes resulting in combinations with *sal^{EPv}-Gal4*, *638-Gal4*, and *shv-Gal4* are shown in Figure 6, F–Q. For example, the combination *s-43/sal^{EPv}-Gal4* affects only the distal region of the wing margin (Figure 6N). The *s-43* line gave a very strong wing-margin phenotype in combination with *638-Gal4* (Figure 6J), and a thickening of the longitudinal veins in combination with *shv-Gal4* (Figure 6F). All these phenotypes are reminiscent of reductions in Notch signaling at the developmental times of Gal4 expression. In other cases, the similarities

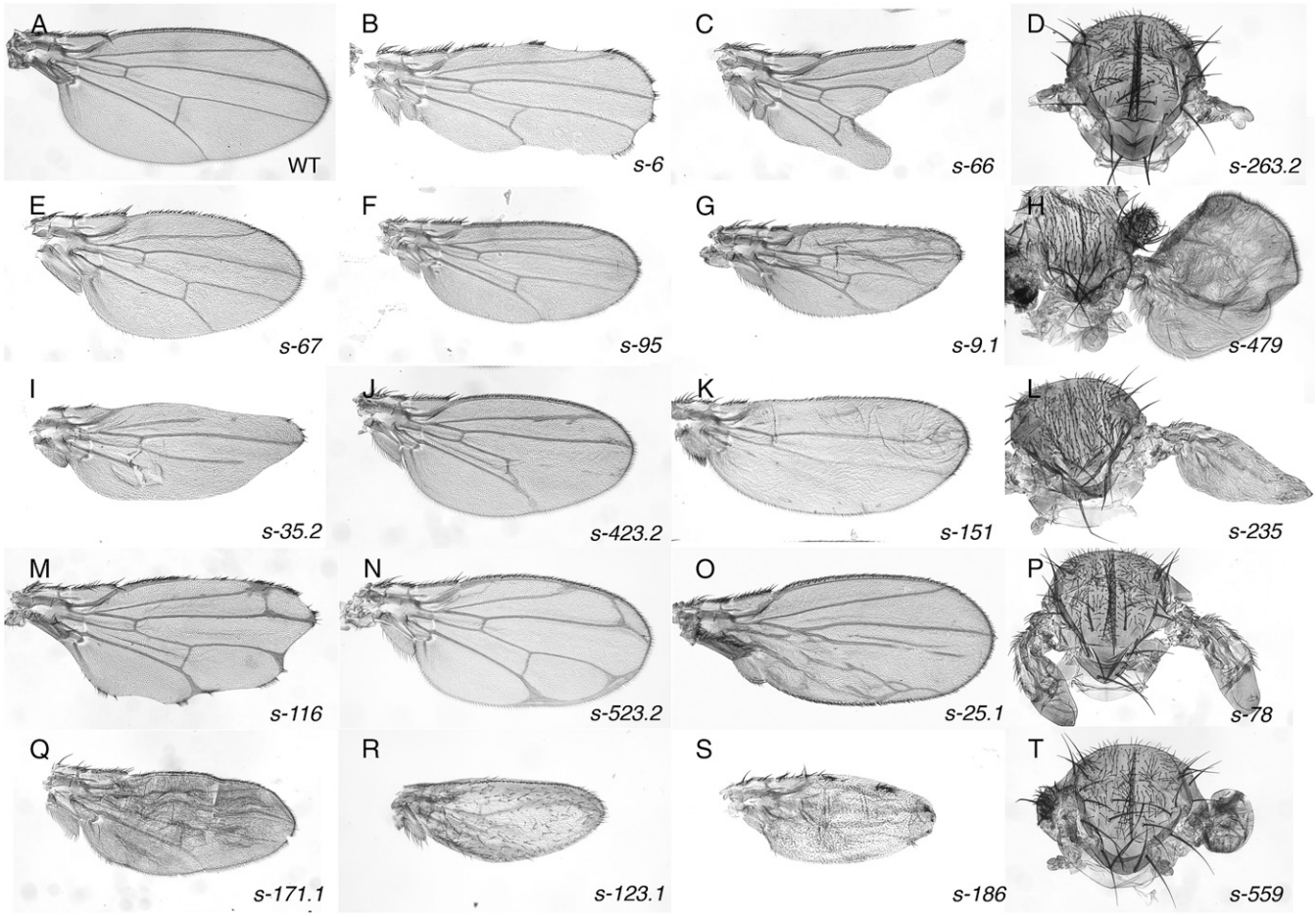

Figure 5.—Wing phenotypes of *P-GS/638-Gal4* combinations. Representative phenotypes observed in combinations between *P-GS* insertions and the *638-Gal4* line. (A) Wild-type wing. (B–D) Weak (B), moderate (C), and strong (C) loss of wing margin and wing tissue. (E–G) Reduced wing size without an effect on vein patterning. (H) Large wing, partially transformed to notum, with extra vein tissue. (I–L) Loss of different longitudinal veins accompanied by loss of wing-margin structures (I and L). (M and N) Differentiation of thicker veins (M) and extra-vein tissue (N). (O and P) Homeotic transformations from posterior to anterior compartment identity (O) and from wing to haltere tissue (P). (Q) Folded wing resulting from a failure in wing expansion. (R) Severe changes in the vein pattern and formation of ectopic margin hairs in the anterior and posterior compartments of the wing pouch. (S) Loss of wing margin and alterations in trichome morphology. (T) Reduced wing size (right wing) and transformation of wing tissue into notum (left wing).

between the phenotypes obtained in the sal^{EPv}*-Gal4*, *638-Gal4*, and *shv-Gal4* combinations were restricted to only a subset of phenotypes, such as loss of veins in the examples shown in Figure 6, G–I, and Figure 6, O–Q, but similar phenotypes in the sal^{EPv}*-Gal4* combinations (Figure 6, O–Q) were accompanied by very different effects on the wing margin in combinations with *638-Gal4* (Figure 6, K–M), suggesting some specificity of the overexpressed genes in different developmental processes. We integrated the phenotypes of the combinations between the *P-GS* lines and several Gal4 drivers to suggest a candidate pathway affected by the overexpression of each candidate gene (see Table 1).

Rescue of wing-size and pattern phenotypes by a reduction in JNK activity: A considerable fraction of wing phenotypes caused by ectopic or increased gene expression are reminiscent of phenotypes caused by the induction of cell death (see Figure 2 and Figure S1). We expect that these phenotypes will be, to some extent, rescued by the suppression of cell death. The activity of the JNK pathway is instrumental in mediating cell death in the wing, and the expression of the JNK phosphatase Puckered (*puc*) is able to suppress both JNK signaling and cell death in a variety of experimental situations (Adachi-Yamada and O'Connor 2002; Kanda and Miura 2004). Consistently, the phenotype caused by the overexpression of *eiger*, a TNF ligand that causes JNK-dependent cell death (Igaki *et al.* 2002) in the sal^{EPv}*-Gal4/s-200* combination, is totally suppressed by the coexpression of *puc* (Figure 7, B and B′). To analyze the component of cell death in the generation of sal^{EPv}*-Gal4/P-GS* wing phenotypes, we compared the wings of these flies with those of the corresponding sal^{EPv}*-Gal4/P-GS; UAS-puc/+* combinations for all *P-GS* insertions (Figure 7). We find that a considerable fraction of sal^{EPv}*-Gal4/P-GS* phenotypes were not modified by the expres-

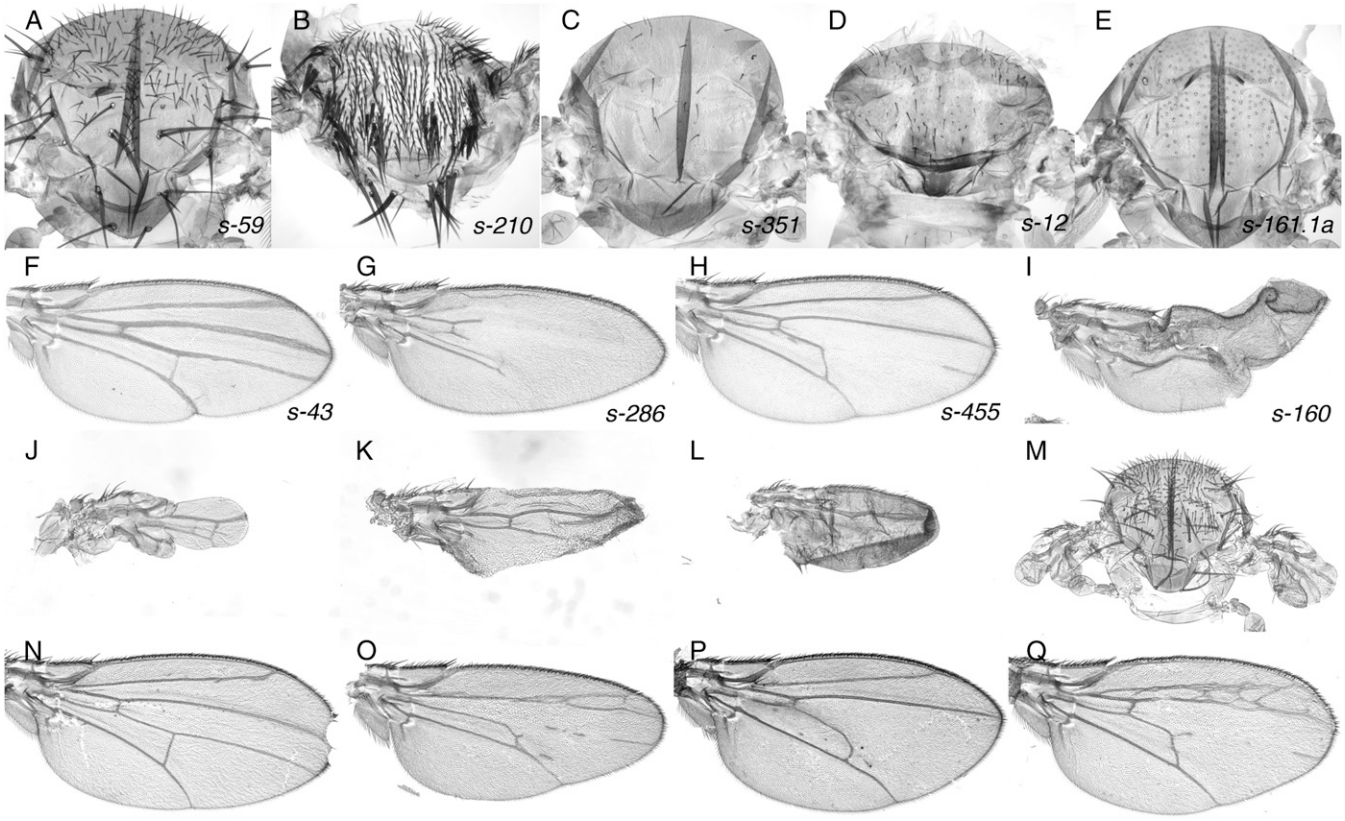

Figure 6.—Thorax and wing phenotype in *P-GS* combinations with Gal4 lines expressed in proneural clusters, the wing disc, and the pupal veins. (A–E) The phenotypes in the thorax were observed in *P-GS/253-Gal4* combinations and consisted of the duplication of macrochaetae (A), the differentiation of clusters of macrochaetae (B), the loss of macrochaetae (C and D), and the loss of tricogen differentiation (E). (F–O) Examples of the wing phenotypes observed in the combinations between the *P-GS* lines *s-43* (F, J, and N), *s-286* (G, K, and O), *s-455* (H, L, and P), and *s-160* (I, M, and Q). The wings in the first row (F–I) correspond to combinations with *shv-Gal4*, the wings in the middle row (J–M) to combinations with *638-Gal4*, and the wings in the bottom row to combinations with sal^{EPv}*-Gal4* (N–Q).

sion of Puc (78%; Figure 7, A′, D, and D′). About 12% of the sal^{EPv}*-Gal4/P-GS* phenotypes were rescued by the simultaneous expression of Puc (Figure 7A′). In these cases, the phenotype of the sal^{EPv}*-Gal4/P-GS; UAS-puc/+* combination corresponds to a milder version of the corresponding sal^{EPv}*-Gal4/P-GS* phenotype (Figure 7, C and C′). In a number of cases, the phenotype of the sal^{EPv}*-Gal4/P-GS* combination was increased by Puc overexpression (10%; Figure 7, A′, E, E′, F, F′, G, G′, H, and H′). In some of these cases, the enhancement is accompanied by the presence of cells that differentiate between the dorsal and ventral wing surfaces (Figure 7, F, F′, G, and G′). It is likely that these cells would have been eliminated by apoptosis in sal^{EPv}*-Gal4/P-GS* wing discs and that the presence of Puc allows them to differentiate after they have delaminated from the imaginal epithelium. Finally, in several cases (5%), the mutant phenotype of the sal^{EPv}*-Gal4/P-GS* combination is not modified by Puc, but the presence of Puc in these backgrounds causes the differentiation of cells located among the dorsal and ventral wing surfaces (Figure 7, H and H′).

To monitor directly the induction of cell death in sal^{EPv}*-Gal4/P-GS* combinations, and to analyze whether the modification of some sal^{EPv}*-Gal4/P-GS* phenotypes by Puc is a consequence of suppressing cell death, we studied the expression of activated Caspase 3, a marker of apoptosis, in several sal^{EPv}*-Gal4/P-GS* and sal^{EPv}*-Gal4/P-GS; UAS-puc/+* genotypes. In two cases, we found a robust and cell autonomous induction of Caspase 3 in sal^{EPv}*-Gal4/P-GS* discs (Figure 8, A′ and C′). The corresponding phenotypes of these combinations, however, were very different (compare A and C in Figure 8), but both were reduced in combination with Puc overexpression (Figure 8, B and D). The suppression of these sal^{EPv}*-Gal4/P-GS* phenotypes by Puc expression is correlated with a reduction of activated Caspase 3 expression in the corresponding imaginal discs (Figure 8, B′ and D′). In contrast, in two cases where the wing phenotype is not associated with the expression of activated Caspase 3 (Figure 8, E and E′, and data not shown), Puc overexpression does not modify the phenotypes of the sal^{EPv}*-Gal4/P-GS* flies (sal^{EPv}*-Gal4/P-GS; UAS-puc/+*; Figure 8, F and F′ and data not shown).

Preliminary characterization of *CG3998*, a gene required for the differentiation of the L5 vein: The *P-GS* line *s-244* causes, in combination with sal^{EPV}*-Gal4*, a

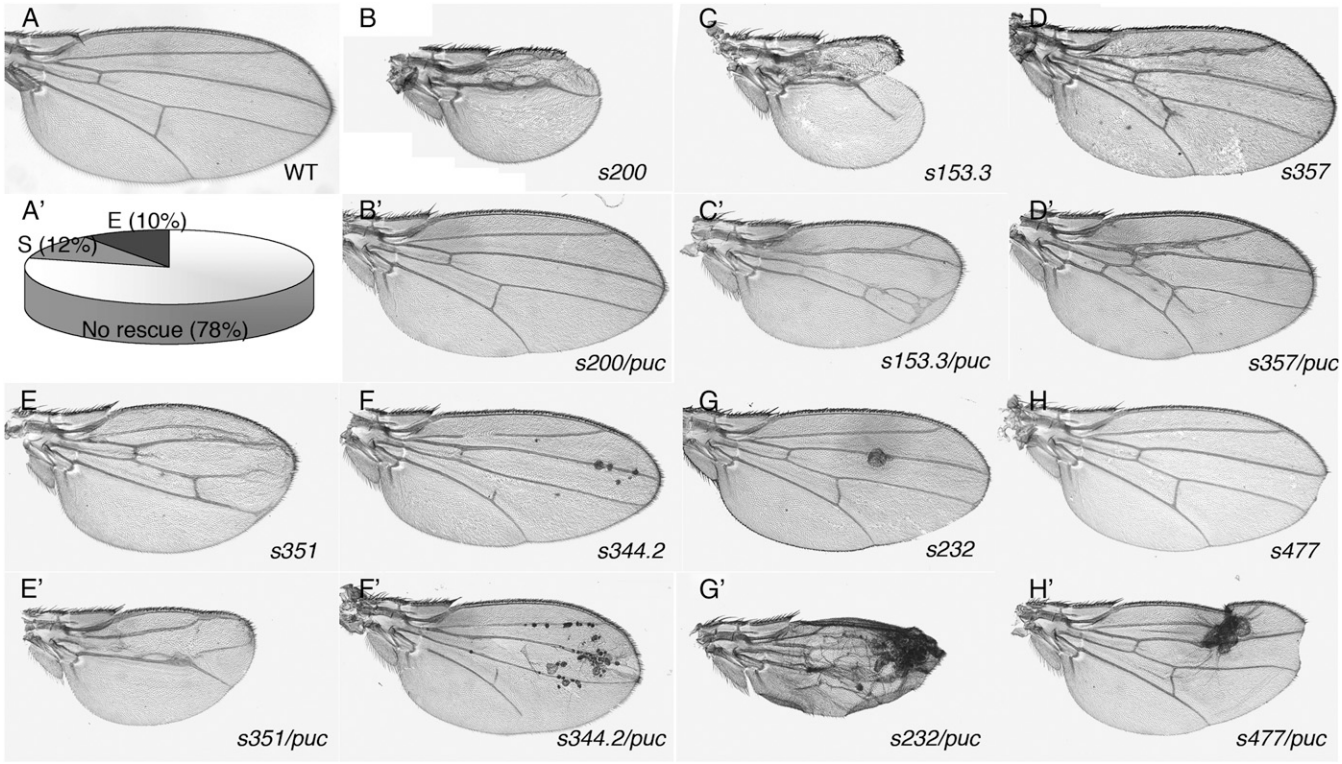

FIGURE 7.—Modifications of *P-GS/sal^{EPv}-Gal4* wing phenotypes by the expression of Puc. (A) Wild-type wing. (A′) Graphic representation of the frequency of *P-GS/sal^{EPv}-Gal4* combinations which phenotype is not modified by Puc ("No rescue"), reduced or **s**uppressed by Puc (S), and **e**nhanced by Puc (E). (B and B′) Example of phenotypic enhancement, visualized in the reduced distance between the veins L2 and L3 and observed in s-*357/sal^{EPv}-Gal4* (B) and *s-357/sal^{EPv}-Gal4; UAS-puc* (B′). (C and D′) Examples of phenotypic rescues by Puc. Partial rescue (C and C′) and total rescue (D and D′). (E–G′) Examples of phenotypic enhancement by Puc without (E and E′) and with a strong increase (F and F′ and G and G′) in the appearance of cells located between the dorsal and ventral wing surfaces. (H and H′) The expression of Puc does not modify the loss of the distal wing-margin phenotype of *s-477/sal^{EPv}-Gal4* wings (H) but causes the formation of trapped cells (H′).

strong phenotype of wing-size reduction and loss of veins in the central region of the wing (Figure 9). The gene most likely causing this phenotype is *CG3998*, encoding a C2H2 zinc (Zn)-finger protein that might regulate gene expression (Zn30C; Figure 9A). pBlast searches identified two related human genes not yet characterized that contain a Zn-finger domain, human Zn-finger proteins 665 and 160 (32% identity with Zn30C). *CG3998* is expressed in all wing cells, and Gal4 regulates its expression in the *s-244* background (Figure 9, B and C). To confirm that *CG3998* causes the phenotypes of *s-244*/Gal4 combinations, we introduced into a *638-Gal4/s-244* genetic background the UAS RNAi lines directed against *CG3998* and the adjacent gene *Cyp4E3*. Only the presence of *UAS-CG3998i* rescues the phenotype of the *638-Gal4/s-244* combination, indicating that this gene is causing the overexpression phenotypes characteristic of *s-244* (compare F and H in Figure 9). The expression of *CG3998* RNAi on its own causes a phenotype of loss of the distal L5 vein (Figure 9F), which is very similar to the phenotype of the loss-of-function alleles in the gene (Figure 9E). In this manner, *CG3998* is normally required for the formation of the L5 vein, and its expression at higher-than-normal levels in the wing interferes with its growth and patterning. Finally, to identify a likely mechanism for the loss-of-function phenotype of *CG3998*, we studied the expression of the *Iroquois* genes (*Iro-C*) in the wing disc. We noted that the characteristic expression of the *Iro-C* in the L5 territory is lost in wing discs expressing the RNAi directed against *CG3998* (Figure 9, I and J).

DISCUSSION

The function of a large fraction of the Drosophila annotated genes is still unknown, and this situation is particularly common in the case of genes encoding proteins without known structural motives or homology to other sequences in the databases. In this way, the identification of genes on the basis of the generation of mutant phenotypes, by either loss- or gain-of-function screens, is instrumental in the assignation of functions to poorly characterized coding regions. In this work, we present the results of a gain-of-function screen that aims to identify genes involved in wing development by using a Gal4 driver expressed in the central region of the wing blade (*sal^{EPv}-Gal4*). Because changes in the activity or expression of members of the Notch-, EGFR-, and Dpp-

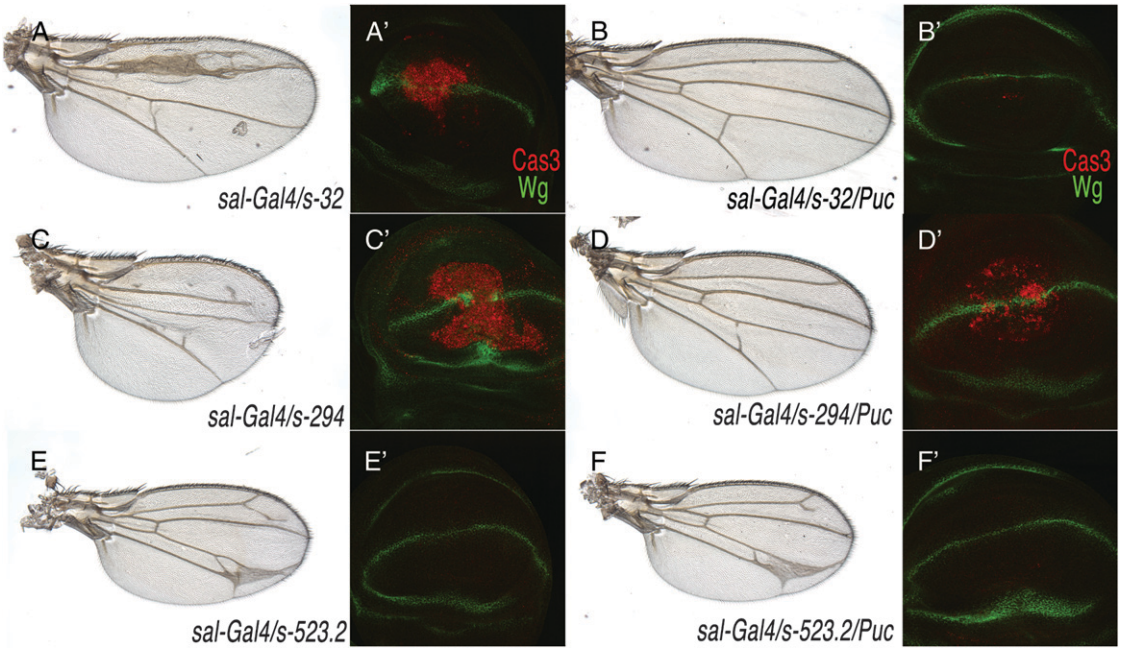

FIGURE 8.—Effects of Puc on wing phenotypes and cell death. In all wing discs, the expression of Wingless (Wg) is in green and the expression of activated Caspase 3 (Cas3) is in red. Discs are oriented with the ventral side up and the anterior side to the left. (A and A′) Wing (A) and the third instar wing disc (A′) of the *sal^{EPv}-Gal4/s-32* genotype (*sal-Gal4/s-32*). Activated Caspase 3 is detected in the center of the wing at both sides of the stripe of Wingless expression. (B and B′) Wing (B) and the third instar wing disc (B′) of the *sal^{EPv}-Gal4/s-32; UAS-puc/+* genotype (*sal-Gal4/s-32/Puc*). The wing phenotype is totally suppressed, and only some remnants of activated Caspase 3 are detected in the ventral compartment. (C and C′) Wing (C) and the third instar wing disc (C′) of the *sal^{EPv}-Gal4/s-294* genotype (*sal-Gal4/s-294*). Caspase 3 is expressed in the entire domain of *sal^{EPv}-Gal4* expression. (D and D′) Wing (D) and the third instar wing disc (D′) of the *sal^{EPv}-Gal4/s-294; UAS-puc/+* genotype (*sal-Gal4/s-294/Puc*). The wing phenotype is partially suppressed, and lower levels of activated Caspase 3 are detected in the domain of *sal^{EPv}-Gal4* expression. (E and E′) Wing (E) and the third instar wing disc (E′) of the *sal^{EPv}-Gal4/s-523.2* genotype (*sal-Gal4/s-523.2*). There is no expression of activated Caspase 3. (F and F′) Wing (F) and the third instar wing disc (F′) of the *sal^{EPv}-Gal4/s-523.2; UAS-puc/+* genotype (*sal-Gal4/s-523.2/Puc*). The wing phenotype is not modified by the expression of Puc.

signaling pathways in the domain of *sal^{EPv}-Gal4* expression cause phenotypes consistent with the known requirement of these pathways, we expected that our screen has the potential to identify additional components of these pathways. In fact, 25 genes targeted by *P-GS* insertions correspond to known members of these pathways (Table S2), including, for example, *N*, *Dl*, *Su(H)*, *gro*, *fng*, and *psq* in the Notch pathway. Another datum validating the screen is that 70% of the candidate genes identified have no previously assigned phenotype in the FlyBase database (see Table 1), and therefore their gain-of-expression phenotypes are the first suggestion of a role during wing development. By comparing these phenotypes with those resulting from manipulations of the Notch, Dpp, JNK, and EGFR pathways, we were able to assign a considerable number of these genes as candidates to modify the activity of these pathways (see Table 1).

Numerical parameters of the screen: The 296 *P-GS* insertions identified correspond to 175 insertion sites and a total of 260 candidate genes. The gene candidates that cause the overexpression phenotype belong to several molecular classes, among which the more numerous correspond to genes encoding transcription factors and other proteins involved in the regulation of gene expression (24%), annotated genes without clear orthologs (29%), and cell-signaling molecules (14%). The proportion of identified genes belonging to these classes in the Drosophila genome is very different (7%, 63%, and 10%, respectively; ADAMS *et al.* 2000), indicating that the candidate genes identified in the screen are not a random sample of the genome, as individual classes are either under- or overrepresented. Although the screen is far from saturation, it has already identified a considerable number of novel candidate genes that participate in wing morphogenesis and that belong to specific molecular classes. Future work will aim to rigorously confirm the identity of each candidate gene and to define their normal requirements by analyzing their expression patterns in the wing disc and the phenotype of loss-of-function conditions. In the case presented in Figure 9, we were able to confirm the identity of the candidate gene (*CG3998*) for a particular insertion (*s-244*) using an RNAi approach and showed that the gene causing the gain-of-expression phenotype is required during the development of the wing for the regulation of Iro-C expression in the L5 vein and for the formation of this vein.

Wing phenotypes and candidate developmental processes affected: We obtained a restricted set of wing

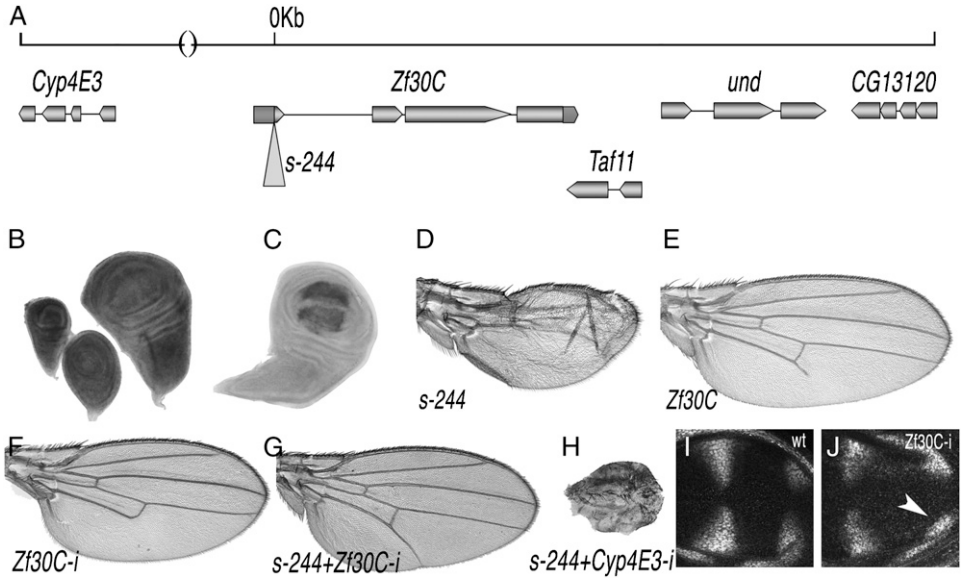

FIGURE 9.—Analysis of *s-244* and its candidate gene *CG3998* (*Znf30C*). (A) Representation of the genomic region where the *P-GS* insertion *s-244* is located. (B and C) *In situ* hybridization of wild type (B) and sal^{EPv}*-Gal4/s-244* (C) third instar discs with a RNA probe of the *Zf30C* gene. (D) Adult wing showing the phenotype of sal^{EPv}*-Gal4/s-244* flies (s-244). (E) Phenotype of the $P\{lacW\}zf30C^{k02506}/l(2)SH1998^{SH1998}$ combination, corresponding to a loss of function of *Zf30C*. (F) Phenotype caused by the expression of RNAi directed against *Zf30C* in *638-Gal4/UAS-iZf30c* females raised at 29°. (G and H) Phenotype of *638-Gal4/s-244* flies expressing the RNAi of *Zf30C* (G) and *Cyp4E3* (H). (I and J) Expression of the Iro-C proteins in the wing blade of wild-type (I) and *638-Gal4/UAS-iZf30C* (J) third instar discs. Only the expression in the L5 vein (arrowhead in J) is lost in the distal region of the presumptive L5 territory.

phenotypes in sal^{EPv}*-Gal4/P-GS* combinations, likely because the timing and expression pattern of the driver is limited to a central domain of the wing blade during the third instar larval stage. Most phenotypes consist of changes in the size and/or the pattern of the wing, mainly smaller-than-normal wings with a different degree of modifications in the spacing between veins. These phenotypes are expected because the miss-expression of a candidate gene coincides with cell proliferation and with the specification of provein and intervein territories in the wing blade. In this manner, misexpression of the candidate genes might interfere with a variety of processes taking place in the wing-blade epithelium during the third larval instar. At this developmental stage, the activities of the Hh- and Dpp-signaling pathways direct the generation of the spatial domains of transcription factor expression, the function of which is involved in wing patterning, and changes in the efficiency of Hh and Dpp signaling cause profound effects in wing morphology similar to those observed in many sal^{EPv}*-Gal4/P-GS* combinations. Similarly, the time of sal^{EPv}*-Gal4* expression includes the time when the EGFR and Notch pathways interact with each other to determine vein commitment and thickness, respectively, and also the time when the Notch and Wg pathways maintain the dorso-ventral boundary and control gene expression along this axes. The sal^{EPv}*-Gal4/P-GS* combinations affecting preferentially the veins or the wing margin might well identify candidate genes regulating these processes. Finally, in addition to a complex set of signaling and transcription activities controlling wing-disc patterning, in the third instar wing disc, cells are engaged in active cell proliferation leading to the acquisition of the characteristic wing-disc size and shape (MILAN *et al.* 1996; BAENA-LOPEZ *et al.* 2005). In addition to cell-cycle regulators, the insulin-, TGFβ-, and Fat/Yorkie-signaling pathways play a key role in controlling cell growth and proliferation (BRUMMEL *et al.* 1999a; HAFEN 2004; REDDY and IRVINE 2008), and perturbations in these activities are expected to modify the size of the wing without severely changing the pattern of veins or sensory organs.

Developmental specificity of gene overexpression in different tissues: The signaling pathways and transcription factors controlling wing development also have requirements in other tissues and developmental processes. This implies that *P-GS* insertions targeting genes affecting signaling pathways should also display phenotypes in other tissues in combination with different tissue-specific Gal4 lines. This is indeed the case, as a large fraction of combinations between *P-GS* insertions and other Gal4 drivers resulted in mutant phenotypes (83% with *ey-Gal4*, 77% with *shv-Gal4*, and 66% with *253-Gal4*). This observation indicates that there are no strong tissue- or developmental-time-specific effects of the identified genes. The high percentage of lethality among *P-GS* combinations with these other drivers validates the use of $sal^{E/Pv}$*-Gal4* in F_1 screenings of *P-GS* insertions.

It is interesting to compare the results of the presented screen with those of a similar screen in which the *P-GS* lines were selected using a Gal4 driver that was expressed only in the developing veins during pupal development (*shv-Gal4*) (MOLNAR *et al.* 2006). In this case, most of the genes identified also affected wing development when the *P-GS* lines were combined with a wing-disc driver. We find that only 46 of the 175 insertion sites identified with sal^{EPv}*-Gal4* were already selected in the previous *shv-Gal4* screen. This corresponds to a percentage of only 27%. Similarly, only 18% of the insertion sites isolated with *shv-Gal4* (from a total

of 262 sites) were again identified in the *sal^{EPv}-Gal4* screen. Although the *shv-Gal4* screen was carried out to higher numbers than the *sal^{EPv}-Gal4* one—13,000 *P-GS* compared to 3440 *P-GS*—the overlap between both screens is very low, suggesting that the characteristics of the Gal4 line used impose severe restrictions on the identity of the isolated *P-GS* insertion sites. The low frequency of redundancy between both screens could be in part a consequence of the lethality of many *shv-Gal4/P-GS* combinations, as 40% of the *P-GS* insertion sites isolated with *sal^{EPv}-Gal4* were lethal in combination with *shv-Gal4*. In contrast, a large fraction of *P-GS* lines isolated with *shv-Gal4* were wild type in combination with *sal^{EPv}-Gal4*, even though they display clear phenotypes in combination with the stronger wing-disc driver *638-Gal4*. In this manner, the expression pattern, developmental time, and strength of the Gal4 line used are key determinants in the likelihood of identifying selectable phenotypes in F_1 experiments.

Wing phenotypes and cell death: We find that a considerable fraction (78%) of *sal^{EPv}-Gal4/P-GS* phenotypes were not modified by the expression of Puc, suggesting that they were not a consequence of cell death caused by gene overexpression, but rather the result of alterations in wing growth and patterning. In ~12% of *sal^{EPv}-Gal4/P-GS* combinations, the phenotype was rescued by the simultaneous expression of Puc. In these cases, we expect that the induction of cell death by gene overexpression in the wing disc is a principal component of the adult phenotype. The phenotypes that were rescued by Puc expression correspond primarily to changes in size and pattern (75%) or in wing size (20%), and none of the phenotypes affecting only vein patterning were modified by the expression of Puc. It is interesting to note that wing discs in which activated Caspase 3 is massively detected in its central domain give rise to very different wing phenotypes, suggesting that not only cell death, but also other effects of the gene causing it, could be instrumental in the generation of particular wing phenotypes. The monographic analysis of the genes identified in this screen along the lines initiated for the *CG3998* gene, should permit defining their specific roles and determine their normal contribution to wing formation.

We are very grateful to A. García-Bellido for his continuous support. C. Molnar, E. Sanchez-Herrero, and A. Baonza are acknowledged for critical reading of the manuscript. Grants from Dirección General de Investigación Científica y Técnica BCM2006-01787 and CONSOLIDER to J.F.dC. and an institutional grant from Fundación Ramón Areces to the Centro de Biología Molecular "Severo Ochoa" are also acknowledged.

LITERATURE CITED

Adachi-Yamada, T., and M. B. O'Connor, 2002 Morphogenetic apoptosis: a mechanism for correcting discontinuities in morphogen gradients. Dev. Biol. **251:** 74–90.

Adams, M. D., S. E. Celniker, R. A. Holt, C. A. Evans, J. D. Gocayne *et al.*, 2000 The genome sequence of Drosophila melanogaster. Science **287:** 2185–2195.

Baena-Lopez, L. A., A. Baonza and A. Garcia-Bellido, 2005 The orientation of cell divisions determines the shape of Drosophila organs. Curr. Biol. **15:** 1640–1644.

Barrio, R., and J. F. de Celis, 2004 Regulation of spalt expression in the Drosophila wing blade in response to the Decapentaplegic signaling pathway. Proc. Natl. Acad. Sci. USA **101:** 6021–6026.

Barrio, R., J. F. de Celis, S. Bolshakov and F. C. Kafatos, 1999 Identification of regulatory regions driving the expression of the *Drosophila spalt* complex at different developmental stages. Dev. Biol. **215:** 33–47.

Bate, C. M., and A. Martinez-Arias, 1991 The embryonic origin of imaginal discs in *Drosophila*. Development **110:** 755–761.

Blair, S. S., 1995 Compartments and appendage development in *Drosophila*. BioEssays **4:** 299–309.

Brand, A. H., and N. Perrimon, 1993 Targeted gene expression as a means of altering cell fates and generating dominant phenotypes. Development **118:** 401–415.

Brogiolo, W., H. Stocker, T. Ikeya, F. Rintelen, R. Fernandez *et al.*, 2001 An evolutionarily conserved function of the Drosophila insulin receptor and insulin-like peptides in growth control. Curr. Biol. **11:** 213–221.

Brummel, T., S. Abdollah, T. E. Haerry, M. J. Shimell, J. Merriam *et al.*, 1999a The Drosophila activin receptor baboon signals through dSmad2 and controls cell proliferation but not patterning during larval development. Genes Dev. **13:** 98–111.

Brummel, T., S. Abdollah, T. E. Herry, M. J. Shimell, J. Merrian *et al.*, 1999b The *Drosophila* Activin receptor Baboon signals through dSmad2 and controls cell proliferation but not patterning during larval development. Genes Dev. **13:** 98–111.

Buff, E., A. Carmena, S. Gisselbrecht, F. Jimenez and A. Michelson, 1998 Signalling by the Drosophila epidermal growth factor receptor is required for the specification and diversification of embryonic muscle progenitors. Development **125:** 2075–2086.

Butler, M. J., T. L. Jacobsen, D. M. Cain, M. G. Jarman, M. Hubank *et al.*, 2003 Discovery of genes with highly restricted expression patterns in the Drosophila wing disc using DNA oligonucleotide microarrays. Development **130:** 659–670.

Calleja, M., E. Moreno, S. Pelaz and G. Morata, 1996 Visualization of gene expression in living adult *Drosophila*. Science **274:** 252–255.

Cohen, S. M., 1993 *Imaginal Disc Development*. Cold Spring Harbor Laboratory Press, Cold Spring Harbor, NY.

de Celis, J. F., 1998 Positioning and differentiation of veins in the *Drosophila* wing. Int. J. Dev. Biol. **42:** 335–343.

de Celis, J. F., 2003 Pattern formation in the Drosophila wing: the development of the veins. BioEssays **25:** 443–451.

de Celis, J. F., and A. Garcia-Bellido, 1994 Roles of the *Notch* gene in Drosophila wing morphogenesis. Mech. Dev. **46:** 109–122.

de Celis, J. F., R. Barrio and F. C. Kafatos, 1996a A gene complex acting downstream of *dpp* in *Drosophila* wing morphogenesis. Nature **381:** 421–424.

de Celis, J. F., A. Garcia-Bellido and S. Bray, 1996b Activation and function of *Notch* at the dorsoventral boundary in the *Drosophila* wing imaginal disc. Development **122:** 359–369.

de Celis, J. F., S. Bray and A. Garcia-Bellido, 1997 Notch signalling regulates *veinlet* expression and establishes boundaries between veins and interveins in the *Drosophila* wing. Development **124:** 1919–1928.

de Celis, J. F., R. Barrio and F. C. Kafatos, 1999 Regulation of the *spalt/spalt-related* gene complex and its function during sensory organ development in the *Drosophila* thorax. Development **126:** 2653–2662.

Diaz-Benjumea, F. J., and S. M. Cohen, 1995 Serrate signals through Notch to establish a wingless-dependent organized at the dorsal/ventral compartment boundary of the *Drosophila* wing. Development **121:** 4215–4225.

Garcia-Bellido, A., F. Cortes and M. Milan, 1994 Cell interactions in the control of size in *Drosophila* wings. Proc. Natl. Acad. Sci. USA **91:** 10222–10226.

Hafen, E., 2004 Interplay between growth factor and nutrient signaling: lessons from Drosophila TOR. Curr. Top. Microbiol. Immunol. **279:** 153–167.

Halder, G., P. Callaerts, S. Flister, U. Walldorf, U. Kloter *et al.*, 1998 Eyeless initiates the expression of both sine oculis and

eyes absent during Drosophila compound eye development. Development **125:** 2181–2191.

Igaki, T., H. Kanda, Y. Yamamoto-Goto, H. Kanuka, E. Kuranaga *et al.*, 2002 Eiger, a TNF superfamily ligand that triggers the Drosophila JNK pathway. EMBO J. **21:** 3009–3018.

Ingham, P. W., and A. P. McMahon, 2001 Hedgehog signaling in animal development: paradigms and principles. Genes Dev. **15:** 3059–3087.

Irvine, K. D., and T. F. Vogt, 1997 Dorso-ventral signalling in limb development. Curr. Opin. Cell Biol. **9:** 867–876.

Ito, K., W. Awano, K. Suzuki, Y. Hiromi and D. Yamamoto, 1997 The *Drosophila* mushroom body is a quadruple structure of clonal units each of which contains a virtually identical set of neurones and glial cells. Development **124:** 761–771.

Kanda, H., and M. Miura, 2004 Regulatory roles of JNK in programmed cell death. J. Biochem. **136:** 1–6.

Lawrence, N., T. Klein, K. Brennan and A. Martinez Arias, 2000 Structural requirements for Notch signalling with Delta and Serrate during the development and patterning of the wing disc of Drosophila. Development **127:** 3185–3195.

Lawrence, P. A., and G. Struhl, 1996 Morphogens, compartments, and pattern: Lessons from *Drosophila*? Cell **85:** 951–961.

Liao, G.-C., E. J. Rehm and G. E. Rubin, 2000 Insertion site preferences of the P transposable element in Drosophila melanogaster. Proc. Natl. Acad. Sci. USA **97:** 3347–3351.

Mann, R. S., and G. Morata, 2000 The developmental and molecular biology of genes that subdivide the body of *Drosophila*. Annu. Rev. Cell Dev. Biol. **16:** 243–271.

Martin, F. A., A. Perez-Garijo, E. Moreno and G. Morata, 2004 The brinker gradient controls wing growth in Drosophila. Development **131:** 4921–4930.

Martin-Blanco, E., A. Gampel, J. Ring, K. Virdee, N. Kirov *et al.*, 1998 puckered encodes a phosphatase that mediates a feedback loop regulating JNK activity during dorsal closure in Drosophila. Genes Dev. **12:** 557–570.

Méthot, N., and K. Basler, 1999 Hedgehog controls limb development by regulating the activities of distinct transcriptional activator and repressor forms of Cubitus interruptus. Cell **96:** 819–831.

Micchelli, C. A., E. J. Rulifson and S. Blair, 1997 The function and regulation of *cut* expression on the wing margin of *Drosophila*: Notch, Wingless and a dominant negative role for Delta and Serrate. Development **124:** 1485–1495.

Milan, M., S. Campuzano and A. Garcia-Bellido, 1996 Cell cycling and patterned cell proliferation in the wing primordium of *Drosophila*. Proc. Natl. Acad. Sci. USA **93:** 640–645.

Mohler, J., M. Seecoomar, S. Agarwal, E. Bier and J. Hsai, 2000 Activation of *knot* specifies the 3–4 intervein region in the Drosophila wing. Development **127:** 55–63.

Molnar, C. and de Celis, J. F., 2006 Independent roles of Drosophila Moesin in imaginal disc morphogenesis and hedgehog signalling. Mech. Dev. **123:** 337–351.

Molnar, C., A. Lopez-Varea, R. Hernandez and J. F. de Celis, 2006 A gain-of-function screen identifying genes required for vein formation in the *Drosophila melanogaster* wing. Genetics **174:** 1635–1659.

Nellen, D., R. Burke, G. Struhl and K. Basler, 1996 Direct and long range action of a DPP morphogen gradient. Cell **85:** 357–368.

Pena-Rangel, M. T., I. Rodriguez and J. R. Riesgo-Escovar, 2002 A misexpression study examining dorsal thorax formation in *Drosophila melanogaster*. Genetics **160:** 1035–1050.

Reddy, B. V., and K. D. Irvine, 2008 The Fat and Warts signaling pathways: new insights into their regulation, mechanism and conservation. Development **135:** 2827–2838.

Rørth, P., 1996 A modular misexpression screen in Drosophila detecting tissue-specific phenotypes. Proc. Natl. Acad. Sci. USA **93:** 12418–12422.

Rulifson, E. J., and S. Blair, 1995 *Notch* regulates *wingless* expression and is not required for reception of the paracrine *wingless* signal during wing margin neurogenesis in *Drosophila*. Development **121:** 2813–2824.

Sotillos, S., and J. F. de Celis, 2006 Regulation of *decapentaplegic* expression during Drosophila wing veins pupal development. Mech. Dev. **123:** 241–251.

Spradling, A. C., D. M. Stern, I. Kiss, J. Roote, T. Laverty *et al.*, 1995 Gene disruptions using P transposable elements: an integral component of the Drosophila genome project. Proc. Natl. Acad. Sci. USA **92:** 10824–10830.

Staehling-Hampton, K., F. M. Hoffmann, M. K. Baylies, E. Rushton and M. Bate, 1994 *dpp* induces mesodermal gene expression in *Drosophila*. Nature **372:** 22–29.

Strigini, M., and S. M. Cohen, 1997 A Hedgehog activity gradient contributes to AP axial patterning of the *Drosophila* wing. Development **124:** 4697–4705.

Struhl, G., and K. Basler, 1993 Organizing activity of wingless protein in Drosophila. Cell **72:** 527–540.

Tabata, T., and T. B. Kornberg, 1994 Hedgehog is a signaling protein with a key role in patterning Drosophila imaginal discs. Cell **76:** 89–102.

Teleman, A. A., and S. M. Cohen, 2000 Dpp gradient formation in the *Drosophila* wing maginal disc. Cell **103:** 971–980.

Toba, G., T. Ohsako, N. Miyata, T. Ohtsuka, K. H. Seong *et al.*, 1999 The gene search system: a method for efficient detection and rapid molecular identification of genes in *Drosophila melanogaster*. Genetics **151:** 725–737.

Tsuneizumi, K., T. Nakayama, Y. Kamoshida, T. Koernberg, J. Christian *et al.*, 1997 Daughters against dpp modulates dpp organizing activity in Drosophila wing development. Nature **389:** 627–631.

Vervoort, M., M. Crozatier, D. Valle and A. Vincent, 1999 The COE transcription factor Collier is a mediator of short-range Hedgehog-induced patterning of the *Drosophila* wing. Curr. Biol. **9:** 632–639.

Walsh, E. P., and N. H. Brown, 1998 A screen to identify Drosophila genes required for integrin-mediated adhesion. Genetics **150:** 791–805.

Wilson, R. J., J. L. Goodman and V. B. Strelets, 2008 FlyBase: integration and improvements to query tools. Nucleic Acids Res. **36:** D588–D593.

Zecca, M., K. Basler and G. Struhl, 1995 Sequential organizing activities of *engrailed*, *hedgehog*, and *decapentaplegic* in the *Drosophila* wing. Development **121:** 2265–2278.

Zecca, M., K. Basler and G. Struhl, 1996 Direct and long-range action of a Wingless morphogen gradient. Cell **87:** 833–844.

Communicating editor: T. Schüpbach

GENETICS

Supporting Information
http://www.genetics.org/cgi/content/full/genetics.109.107748/DC1

A Gain-of-Function Screen Identifying Genes Required for Growth and Pattern Formation of the *Drosophila melanogaster* Wing

Cristina Cruz, Alvaro Glavic, Mar Casado and Jose F. de Celis

DOI: 10.1534/genetics.109.107748

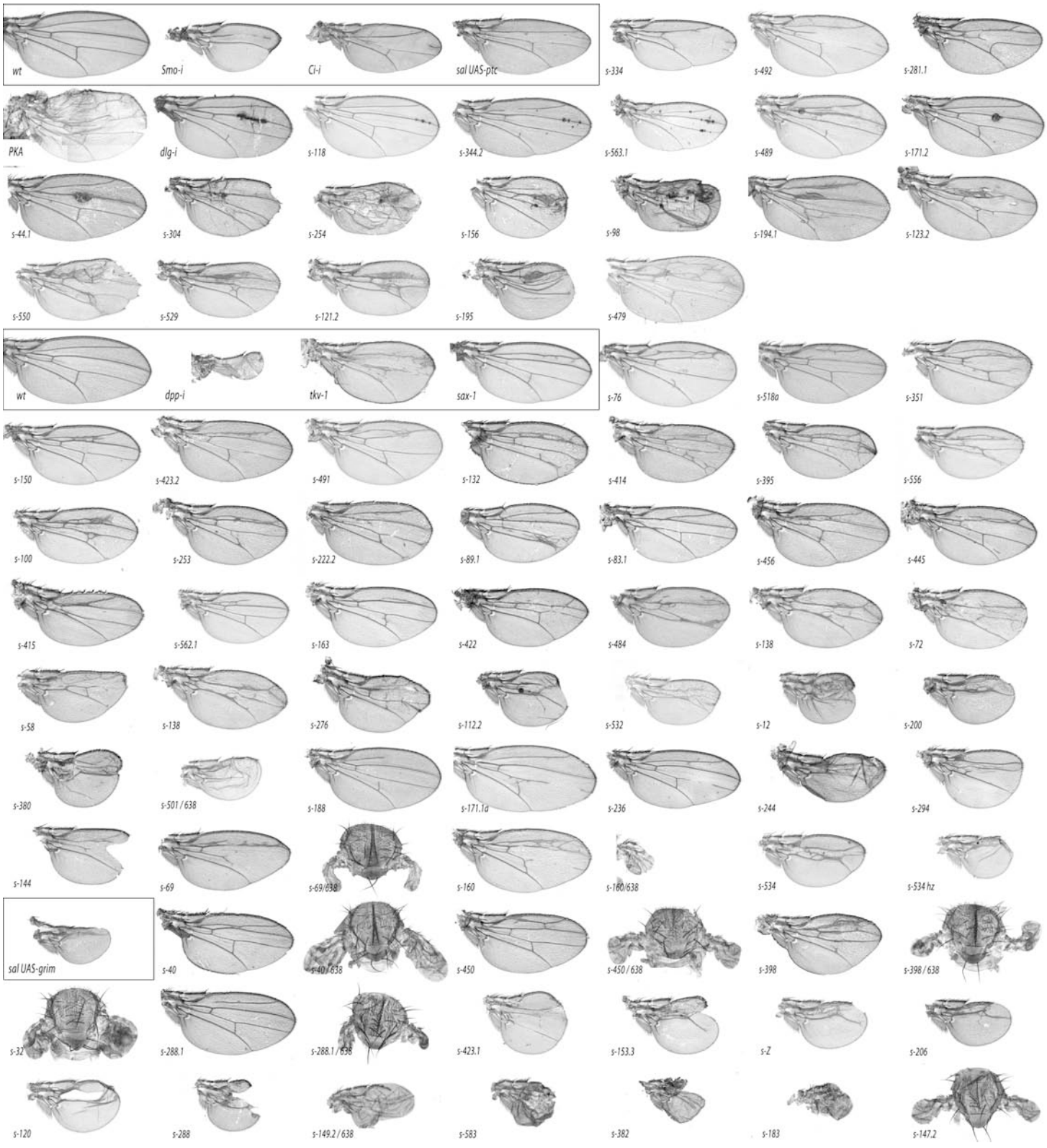

FIGURE S1.—Representative wings of *sal^{EPv}-Gal4/P-GS* or *638-Gal4/P-GS* combinations grouped by similarity to the phenotype caused by alterations in different signalling pathways. Control wings in which individual iRNA directed against some of the known members of these pathways are expressed in the wing blade (638-Gal4) are also shown for *Smoothened (Smo)*, *Cubitus interuptus (Ci)*, *disc large (dlg)*, *dpp*, *thick veins* (*tkv*) and *saxophone* (*sax*). Other control wings correspond to over-expression of wild type genes (Ptc and grim), and mosaic wings in which the function of the gene is eliminated in the wing blade (Pka) in *638-Gal4/+; FRT40 Pka /FRT40 M(2)z; UAS-FLP/+* mosaics. Unless otherwise stated in the Figure, all combinations correspond to P-GS lines and *sal^{EPv}-Gal4*. Rows 1-4: Phenotypes related to Hh signalling with changes in the L3 vein and epithelial integrity. Rows 5-11: Phenotypes related to Dpp signalling with changes in vein spacing and differentiation, and wing size. Rows 12-14 Phenotypes likely related to the induction of cell death.

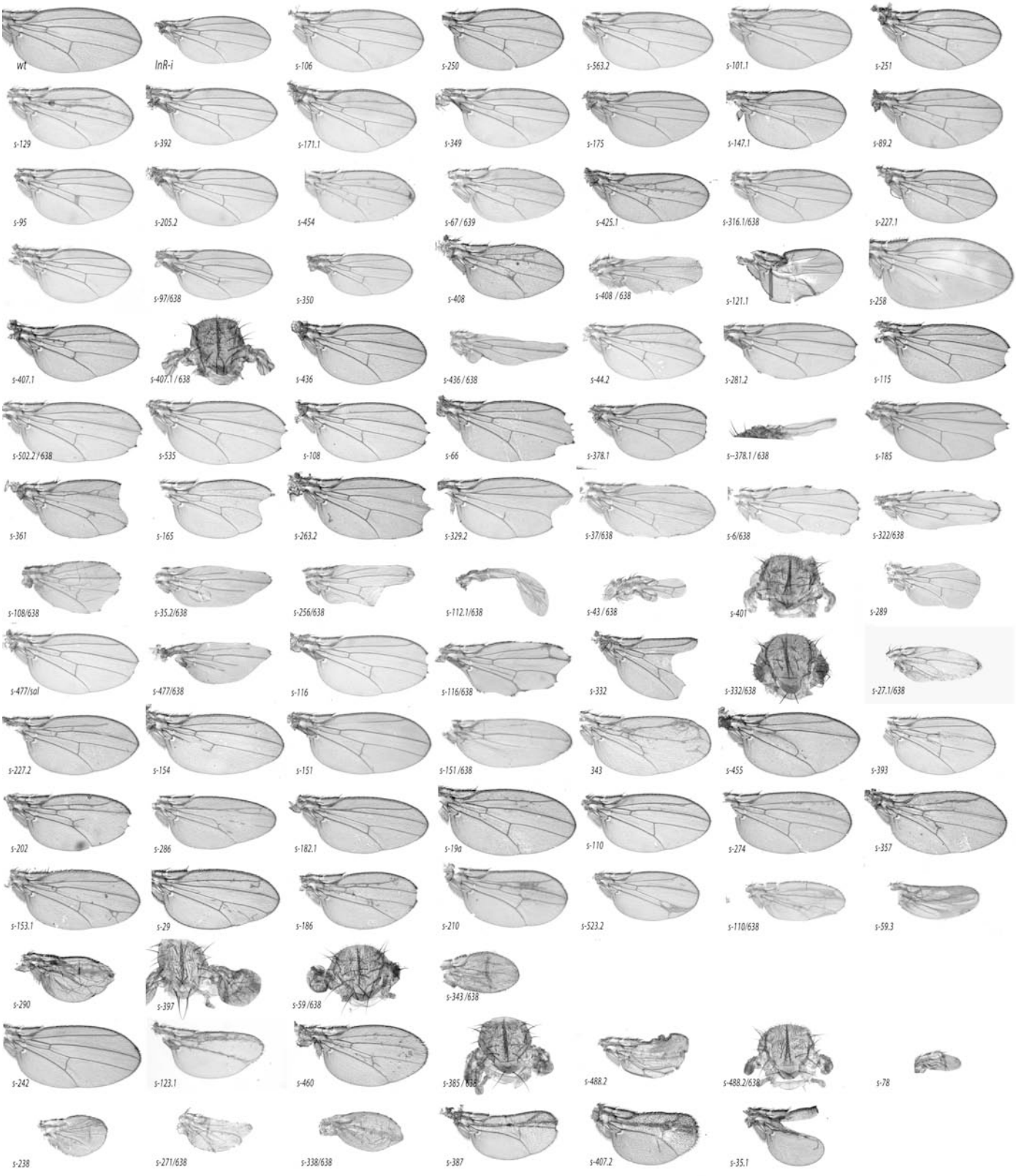

FIGURE S2.—Representative wings of *sal*^{EPv}*-Gal4/P-GS* or *638-Gal4/P-GS* combinations grouped by similarity to the phenotype caused by alterations in different signalling pathways. Control wing in which InR iRNA is expressed in the wing blade (*638-Gal4*) is also shown in row 1. Unless otherwise stated in the Figure, all combinations correspond to P-GS lines and *sal*^{EPv}*-Gal4*. Rows 1-4: Phenotypes related to InR signalling with changes in the size of the wing. Rows 5-9: Phenotypes related to Notch signalling with loss of wing margin structures. Rows 10-13 Phenotypes related to EGFR signalling consisting in loss or gain of veins. Rows 14 and 15 are other phenotypes including the formation of extra bristles in the wing blade (Wingless signalling), homeotic transformations towards haltere, and changes in cell size and trichome number (cell cycle regulators).

TABLE S1

Individual P-GS insertions mapped and the genomic sequences recovered after inverse-PCR

Table S1 is available for download as an Excel file at http://www.genetics.org/cgi/content/full/genetics.109.107748/DC1.

TABLE S2

Identified candidate genes corresponding to transcription factors required in wing formation (Transcription), known components of signalling pathways (Signalling), and other genes related to cytoskeleton dynamics (Cytoskeleton).

P-GS (nº)	Cytology	*sal-Gal4*	Nº	Gene	D	Pathway
Transcription						
s-238 (3)	59F1	S		*CG5393 (apt)*	0	¿?
s-398 (1)	1B7	S-P, CS	2	*CG4262 (elav)*	0	CD
s-147.2 (9)	13F1	S	1	*CG8544 (sd)*	0	CD
s-423.1 (1)	102C2	S-P	0	*CG1449 (zfh2)*	19	CD
s-244 (1)	30C7	S-P, B	1	*CG3998 (zf30C)*	0	Dpp
s-182.1 (1)	67E6	S	1	*CG32067 (simj)*	0	Dpp
s-69 (1)	60B4	V-, Nw	2	*CG3924 (Chi)*	1	Dpp (¿?)
s-380 (1)	50E1	S-P	2	*CG8367 (cg)*	0	Dpp/CD
s-484 (1)	65A4	S-P	2	*CG6586 (tan)*	0	Dpp/CD
s-123.1 (1)	31D11	S-P, +q	1	*CG5102 (da)*	0	Dpp/Wg*
s-29 (1)	68A1	V+	1	*CG12296 (klu)*	0	EGFR*
s-110 (1)	87D8	S	1	*CG7583 (CtBP)*	0	EGFR*
s-143 (2)	88B1	S-P	1	*CG8651 (trx)*	0	Hox
s-262 (3)	35D1	S	1	*CG3758 (esg)*	1	InR
s-97 (1)	55B9	S	2	*CG5738 (lolal)*	0	InR
s-250 (1)	35F1	S	2	*CG7664 (crp)*	0	InR (¿?)
s-401 (4)	17C3	Ns	1	*CG6500 (Bx)*	1	Notch
s-339 (3)	57A6	Nw, S-Pw	2	*CG13425 (bl)*	0	Notch
s-185 (2)	89B9	Nw	1	*CG6889 (tara)*	0	Notch
s-329.2 (2)	86E5	N	1	*CG17228 (pros)*	0	Notch (*)
s-60 (2)	33A1	S-Pw	1	*CG14938 (crol)*	0	Notch/Wg
Signaling						
s-387 (1)	50A13	S-P, CD	2	*CG6033 (drk)*	0	CC (EGFR)
s-127 (5)	100D1	S-P	1	*CG11558 (ttk)*	0	CD (EGFR)
s-32 (1)	29A1	S-P	1	*CG8049 (Btk29A)*	0	CD (JNK)
s-367 (2)	47D6	S	1	*CG7734 (shn)*	0	Dpp (DPP)
s-236 (1)	28D3	V-	2	*CG7233 (snoN)*	1	Dpp (DPP)
s-501 (2)	7B1	S	1	*CG9653 (brk)*	4	Dpp (DPP)
s-200 (1)	46E1	S-P	2	*CG12919 (egr)*	5	Dpp/CD (JNK)
s-132 (1)	35D1	S-Pw	1	*CG11861 (gft)*	1	Dpp/CD (HH)
s-160 (1)	54C12	V-, S	2	*CG4943 (lack)*	0	Dpp/Notch (DPP)
s-89.1 (1)	96F10	S-Pw	1	*CG8384 (gro)*	0	Dpp/Wg* (NOTCH/EGFR)
s-411 (1)	75F6	V-	1	*CG14080 (Mkp3)*	1	EGFR (EGFR)
s-85.1 (1)	94E10	S	2	*CG17077 (pnt)*	0	EGFR (EGFR)
s-59.3	90C1	V+w	2	*CG7467 (osa)*	0	EGFR* (EGFR)

s-503 (1)	94E1	V-	1	*CG4637 (hh)*	0	Hh* (HH)
s-479 (2)	46D4	V	2	*CG15862 (Pka-R2)*	1	Hh* (HH)
s-44.1 (1)	30C5	Ew	3	*CG4379 (Pka-C1)*	0	Hh*/Moe (HH)
s-350 (1)	34C3	S	1	*CG9239 (B4)*	0	InR (INR)
s-147.1 (1)	66A21	S	3	*CG7892 (nemo)*	1	InR/* (WG)
s-357 (2)	47A13	V+, S	1	*CG2368 (psq)*	0	Notch (NOTCH)
s-263.2 (1)	78A1	N	1	*CG10580 (fng)*	0	Notch (NOTCH)
s-70 (1)	92A2	B, V-	1	*CG3619 (Dl)*	1	Notch (NOTCH)
s-361 (1)	21B2	N, S-Pw	1	*CG18497 (spen)*	0	Notch (NOTCH/EGFR)
s-502.2 (1)	3C7	S-Ps, CD	2	*CG3936 (N)*	1	Notch (NOTCH)
s-161.1a (2)	35B8	V-	2	*CG3497 (Su(H))*	1	Notch*/EGFR (NOTCH)
s-289 (1)	3A8	S	1	*CG2621 (sgg)*	0	Wg (WG)
Cytoskeleton						
s-232 (1)	8B6	S, Ew	1	*CG10701 (Moe)*	0	¿?
s-294 (1)	18E1	S-P	2	*CG12530 (Cdc42)*	1	CD
s-112.2 (3)	53E10	S-P	1	*CG9635 (RhoGEF2)*	1	Dpp/CD
s-19a (2)	5C7	V+w	1	*CG4027 (Act5C)*	0	EGFR*
s-281.1 (1)	94E9	S-P	2	*CG6759 (cdc16)*	1	Hh
s-98 (2)	54C12	E, S	2	*CG6477 (RhoGAP54D)*	0	Moe
s-186 (1)	63D1	S	1	*CG12008 (kst)*	15	Notch/¿?
s-332 (1)	57B16	Ns	2	*CG3722 (shg)*	0	Notch/Wg

The "Pathway" column indicates the similarity of the over-expression phenotypes to specific pathways. CD: Cell death. CC: Cell Cycle, InR: Insulin receptor pathway, Dpp: Decapentaplegic pathway. Wg: Wingless pathway. Hh*/Moe: Changes in Hedgehog signalling associated to epithelial defects typical of *moesin* alleles (MOLNAR and DE CELIS, 2006). ¿?: unassigned. The asterisks (*) indicate that the phenotype of over-expression correspond to the activation of the pathway. In the pathway column, and in brackets, is shown the actual pathway to which each candidate genes belong.